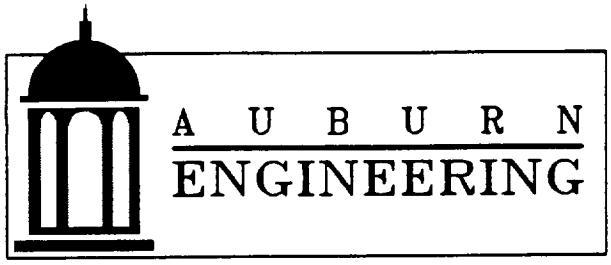


# Crystal Growth Furnace Safety System Validation

Contract NASA–NAS8–39131–DO6

## Final Report

D.W. Mackowski, R. Hartfield, S.H. Bhavnani

and

V.M. Belcher

*College of Engineering*

*Auburn University, AL 36849*

# Crystal Growth Furnace

# Safety System Validation

Contract NASA–NAS8–39131–DO6

## Final Report

4 March 1994

D.W. Mackowski[1], R. Hartfield[2], S.H. Bhavnani[3]

and

V.M. Belcher[4]

Auburn University, AL 36849

[1] Assistant Professor, Mechanical Engineering Department
[2] Assistant Professor, Aerospace Engineering Department
[3] Associate Professor, Mechanical Engineering Department
[4] Graduate Research Assistant

## Report Summary

Reported here are our findings regarding the safe operation of the NASA crystal growth furnace and potential methods for detecting containment failures of the furnace. The main body of the report is taken from the MS thesis of Valerie M. Belcher, whose research task as a graduate student was to investigate the CGF safety problem. The main conclusions of our work are summarized as follows.

1. Ampoule Leak Detection

After an extensive search of the available leak detection methods, we did not identify a quantitative sensor that could feasibly reside within the cartridge and unambiguosly detect the failure of the ampoule. By quantitative, we mean a sensor that detects directly the presence of the crystal growth species. Although several candidate methods were identified, such as absorption and emission spectroscopy, mass spectrometry, gas chomatography, and electrochemical sensors, application of the existing technology to the cartridge environment would have required extensive redesign of the cartridge and/or furnace.

We examined the thermodynamic and mass transfer issues which will affect the performance of qualitative ampoule leak detection methods, such as make– or break–wire sensors. Here, the sensing of the ampoule failure is contingent on the deposition of crystal sample vapor onto the sensor, and the presence of the species is registered by a change in the sensors electrical resistivity. The performance of such sensors will depend to a large extent on the transport and thermodynamic mechanism which govern the motion and deposition of the sample vapor within the cartridge. In the buoyancy–free working environment of the CGF, the transport of the vapor will be governed entirely by diffusion, and deposition will occur on surfaces that are lower that the prevailing dew point temperature of the vapor. An analysis of diffusion–limited vapor transport in a cylindrical cartridge indicates that the vapor will not become significantly supersaturated. That is, one would not expect diffusion to carry the vapor into regions of the cartridge that are cooler than the vapor dew point temperature. Because of this, we would expect in the weightless environment that the deposition of sample vapor originating from a broken ampoule would occur essentially at a single axial location of the cartridge, i.e., the point at which the cartridge and vapor dew point temperatures are equal. This conclusion has important consequences with regard

to the design and placement within the cartridge of a deposition sensor. For example, a sensor located at the cartridge cap would not be expected to perform adequately, because almost all of the sample vapor will have deposited onto the cartridge walls and internal surfaces before reaching the cooled cap. In addition, under earthbound conditions natural convection in the highly nonisothermal cartridge would be expected to significantly alter the vapor transport from the diffusion–limited mode encountered in orbit. Consequently, caution must be exercised in the interpretation of ground–based tests of deposition–based ampoule failure sensors.

Our thermodynamic analyses also indicate that the release of sample vapor into the cartridge from a failed ampoule could, during experimental processing, result in an appreciable increase in the cartridge pressure. Exposure of the molten sample compound will result in the vaporization of the volitile species of the compound. In the case of GaAs, for example, arsenic is the volitile species at the melting temperature. Because the vaporization rate from a free liquid surface is expected to be significantly faster than the rate at which diffusion removes the vapor from the surface, the partial pressure of the vapor species will attain a value governed by the phase equilibria of the liquid–vapor system, and the vapor pressure would be expected to remain at this value for all points in the cartridge that are above the vapor dew point temperature. The increase in total pressure within the cartridge will depend on the sample vapor pressure, the temperature profile in the cartridge, and the volume of the cartridge occupied by the vapor.

Calculations performed using the experimental materials and conditions of USML–1 indicate that, during processing, an ampoule failure could result in a cartridge pressure increase from 42% (for CdZnTe) to 216% (for HgCdTe). This significant increase in pressure suggests that a pressure gauge mounted inside the cartridge could serve as a method for detecting ampoule failure during experimental processing. Although the pressure in the cartridge will increase during the heat–up of the experiment, the normal change in pressure arising from temperature changes could be calibrated into a pressure–based detection scheme system.

2. Cartridge Leak Detection

The objective here is to provide a method that could, first, gauge the integrity of the cartridge independent of whether or not the ampoule itself is broken, and second, identify which cartridge (out of all present in the CGF) has failed. Initially we examined tracer

gas techniques. The approach here is to include a tracer species either within or outside the cartridge, and detect its presence on the opposite side of the cartridge wall. Potential candidate methods were perfluorocarbon tracers, detected with a gas chromatograph, and radioisotopes, detected with an ionization detector or scintillation counter. For the same reasons that eliminated the use of quantitative ampoule failure detection methods, it is not feasible to locate the tracer detector within the cartridge, and it would be necessary to include the tracer within the cartridge and detect its presence in the EAC. This implies that the tracer technique could not identify the specific failed cartridge, unless one employed the unlikely strategy of a different tracer and detection scheme for each cartridge.

An alternative and considerably simpler cartridge detection scheme involves the sensing of a cartridge failure by detecting an anomalous change in cartridge pressure. An analytical model, based on Fanno flow, was developed to predict the rate change in cartridge pressure occuring from a breach of a given size in the cartridge wall. For the EAC and cartridge pressure conditions on USML–1, our results indicate that a 0.01 mm hole in the cartridge would result in a 2% change in cartridge pressure in the order of 0.2 - 5 seconds. This change in pressure could be readily identified with ordinary, piezoresistive pressure sensors, and would also occur much more rapidly than pressure changes associated with normal changes in temperature. A comparison of the pressure based detection method with tracer methods was performed, and we concluded that the amount of tracer in the cartridge that would be required to detect a leak following a 2% decrease in cartridge pressure is unreasonable large – on the order of 10% tracer. The problem with tracers is that the tracer gas is significantly diluted in the EAC following leakage from the ampoule. The pressure gauge method, on the other hand, requires only that a pressure differential exist between the cartridge and the EAC. We should note that for USML–1 this pressure differential is not appreciably large – 98 atm in the EAC vs. 1 atm in the cartridge – yet the response times of the pressure method are still relatively small. A significant improvement in the reponse times of the pressure method could be realized by increasing the EAC–cartridge pressure differential.

3. Detection of Hazardous Species in the EAC

Opening of the EAC may be necessary in future mission to inspect and/or exchange sample cartridges. To permit safe opening, it will be neccessary to insure that toxic species

are not present in hazardous concentrations in the EAC atmosphere. The current method for detecting vapor–phase species in the EAC relys on the visual inspection for vapor deposition onto a cooled mirror plate. This method cannot distinguish between non–toxic and toxic compounds that may be present in the EAC, nor can it determine the concentration of the compounds. Because of these problems, the feasiblity of applying quantitiative measurement methods to detection of sample species in the EAC was performed. The objective of these methods would be to determine both the concentration and composition of vapor compounds within the EAC. Mass spectrometry, while providing extremely high measurement sensitivity and resolution, requires that the samples be injected into essentially a vacuum. This would likely involve modification of the EAC plumbing so that samples could be withdrawn to either a vacuum pump or a detector exposed to the space environment. A more feasible method is spark–source emission spectroscopy. In this technique, an intermittent spark is used to generate a plasma. Vapor species within the plasma will emit radiation at discrete spectral lines. By examining the spectra with a polychomator, the atomic composition and concentration of the species can be determined. For application in the CGF, it would be necessary only to include the spark source mechanism within the EAC, and the radiation from the spark could be optically routed to an externally–located polychomator. In commercial applications, spark source emission spectroscopy is capable of detecting sub parts–per–million concentrations of the common elements associated with crystal growth experiments (As, Hg, Cd etc.). A forseable problem in the method would be the radio frequency noise generated by the spark, which could interfere with the controls and instrumentation in the CGF.

# Appendix I

QUANTITATIVE AND QUALITATIVE LEAK DETECTION METHODS FOR THE CRYSTAL GROWTH FURNACE

Valerie Michelle Belcher

Certificate of Approval:

| | |
|---|---|
| Daniel W. Mackowski<br>Assistant Professor<br>Mechanical Engineering | Sushil H. Bhavnani, Chair<br>Associate Professor<br>Mechanical Engineering |
| Roy J. Hartfield<br>Assistant Professor<br>Aerospace Engineering | Norman J. Doorenbos, Dean<br>Graduate School |

QUANTITATIVE AND QUALITATIVE LEAK DETECTION METHODS FOR THE CRYSTAL GROWTH FURNACE

Valerie Michelle Belcher



_____

Signature of Author

_____

Date

Copy sent to:

Name Date

# VITA

Valerie Michelle Belcher, daughter of Samuel Duval and Carol [redacted] Belcher, was born [redacted] in [redacted]. She graduated from Pensacola Catholic High School in 1986, and then attended Rice University until August of 1987. After transferring to Auburn University in September of 1987, she began work for Marshall Space Flight Center as a cooperative education student in September of 1989, continuing until her graduation. She graduated with a Bachelor's of Mechanical Engineering in June of 1992, and began graduate studies at Auburn University that same month to pursue her Master's of Science, also in mechanical engineering.

THESIS ABSTRACT

# QUANTITATIVE AND QUALITATIVE LEAK DETECTION METHODS FOR THE CRYSTAL GROWTH FURNACE

Valerie M. Belcher

Master of Science, March 18, 1994
(B.M.E., Auburn University, 1992)

118 Typed Pages

Directed by Sushil H. Bhavnani

Recent applications of the Crystal Growth Furnace onboard Spacelab have enabled researchers to study crystallographic solidification processes under microgravity environments. Many of the crystal materials used in previous experiments, and those planned for future missions, are extremely toxic (i.e. Hg, As, Cd) and pose serious hazards to both personnel and hardware. Of primary concern is the safety of shuttle or station crew, as exposure to such compounds could be lethal. Additionally, these materials are volatile at the experimental processing temperatures, and deposition of the crystal compounds onto CGF instrumentation could

necessitate costly repairs, including returning the assembly to earth. Although the current design supplies three distinct levels of containment, there is no suitable method of detecting if one of these levels has failed.

In addressing these issues, the investigation has focused on identifying methods for sensing both ampoule and cartridge failure, and for quantitatively detecting the presence of sample vapors within the EAC. The CGF environment presents leak detection challenges that are not normally encountered under earth-bound situations. The methods cannot involve a high degree of complexity, yet the identification of a leak must be unambiguous. Cartridge and ampoule leak sensors must be sufficiently compact to reside within the cartridge, and must be capable of withstanding high temperatures. Furthermore, the method cannot interfere in any way with the experiment or present a safety hazard in itself.

In the course of this investigation, numerous leak detection methods, both quantitative and qualitative in nature, were evaluated for potential use in the CGF environment. Response times for pressure measurement techniques and detection ability of sensors relying on the direct deposition of a sample material were estimated using Fanno flow and thermodynamic analyses.

TABLE OF CONTENTS

LIST OF TABLES

LIST OF FIGURES

# 1.0 INTRODUCTION

## 1.1 Background

Recent interest in the field of microgravity science has prompted the development of experiments, such as the Crystal Growth Furnace (CGF), to fully capitalize on the microgravity (μg) environment onboard the National Aeronautics and Space Administration's (NASA) space shuttle. A modular, rack-mounted facility, the CGF is used to determine how the absence of gravity-driven convection affects vapor transport and directional solidification processes. Many of the crystal materials used on previous flights, and those planned for future missions, are both extremely toxic (ie. Hg, As, Cd), and have significant vapor pressures at the processing temperatures. These characteristics affect the experiment's implementation on future shuttle flights, and possible long-term experimentation onboard Space Station Freedom (SSF).

Originally, the CGF was located in the cargo bay of the shuttle. Not being environmentally contained within the crew's atmosphere, leakage of the toxic species was of no concern. Yet eventually, as various flight modifications took place, the CGF was moved to a location

inside the Spacelab module where it would require manual manipulation by the crew. Leak detection and species containment have now become paramount concerns, as exposure to such compounds could be lethal. Additionally, deposition of the crystal compounds onto CGF instrumentation could necessitate costly repairs, including returning the assembly to earth.

## 1.2 Experiment Description

The CGF is a reusable facility capable of processing up to six crystal growth samples automatically, at temperatures reaching 1600 °C. The main element of the CGF, the Integrated Furnace Experiment Assembly (IFEA), consists of the Experiment Apparatus Container (EAC), a mechanical Sample Exchange Mechanism (SEM) that rotates a new sample into position, and a Reconfigurable Furnace Module (RFM). A schematic of this configuration is shown in Figure 1. In addition to furnishing the primary structural support, the EAC also provides containment for an argon gas atmosphere and houses the internal experiment hardware. A sample insertion port is included on the EAC for manual sample exchange for missions where more than six samples are scheduled.

In the current design, the samples are contained within a quartz ampoule which, in turn, is secured inside a thin metal cartridge. The sample/ampoule cartridge

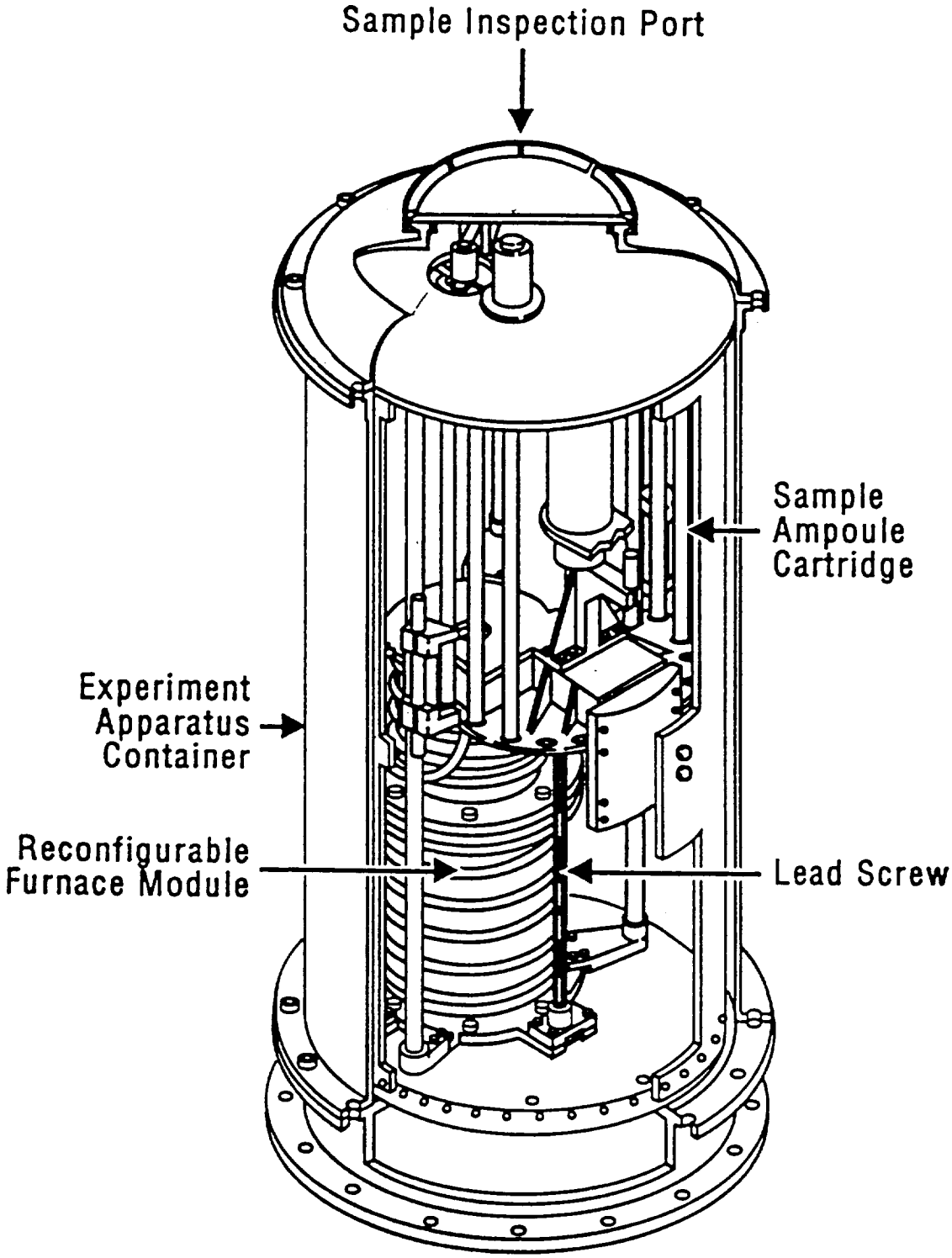


Figure 1: Integrated Furnace Experiment Assembly (IFEA)

(NASA/MSFC, SP-DOC-6102, March 1990)

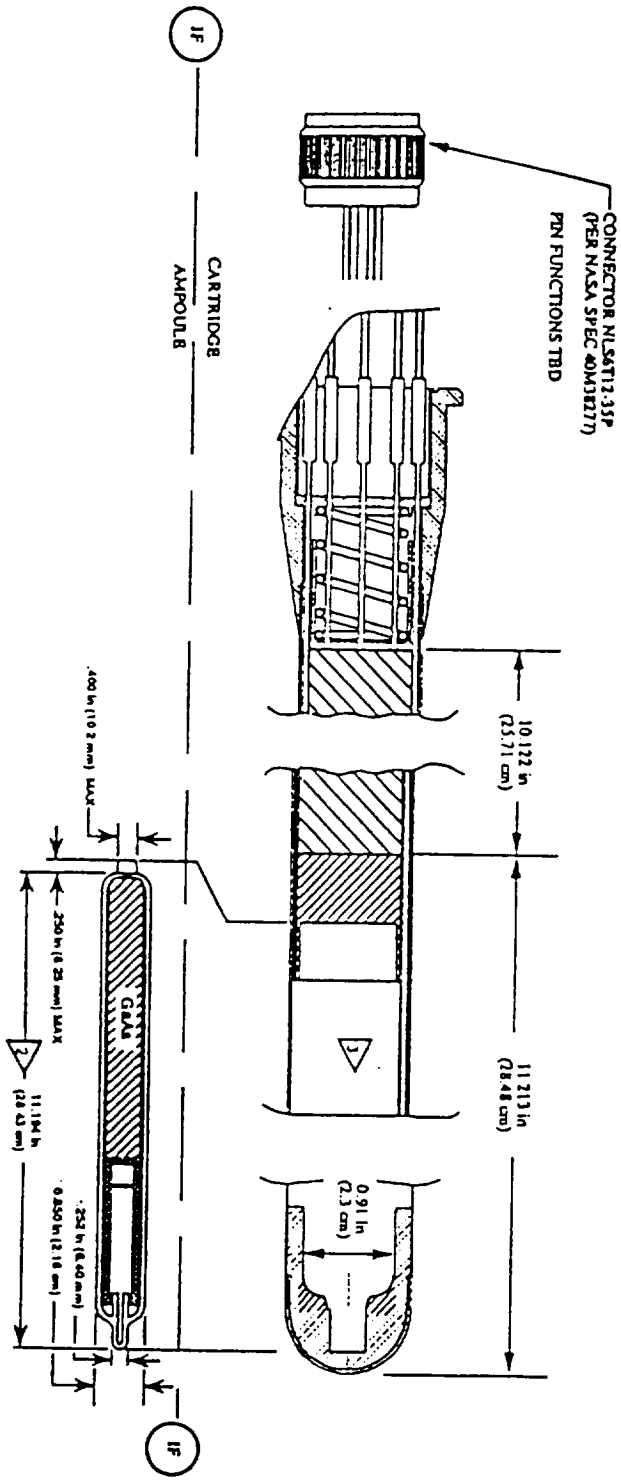


Figure 2: Sample/Ampoule Cartridge Assembly (SACA)

(NASA/MSFC CID-2-60027, March 1990)

assembly (SACA), shown in Figure 2, is held immobile by the SEM while the furnace is vertically translated over the sample being processed, thus avoiding acceleration-induced defects during crystallization. In addition, the system allows precise control of melting and crystal growth conditions.

The furnace itself is comprised of a hot zone, an insulated or adiabatic zone, and a cold zone. An illustration of the RFM is shown in Figure 3. The center 14cm of the cold zone and the center 20cm of the hot zone, both measured in the radial direction, are isothermal to ±1.0%, therefore preventing appreciable nonuniformity of heating within a sample. Additionally, the RFM may be modified between flights by changing the adiabatic zone length to create different heating gradients.

In accordance with current safety certification requirements, the CGF facility has three levels of containment: the combined SACA, the negative pressure in the EAC relative to the Spacelab environmental pressure, and the EAC itself. Although this provides three distinct levels of fault tolerance, the design has several limitations. First, there is no method of detecting the failure of an individual ampoule and/or its cartridge. Thus, if processing were to occur on a failed SACA, the elevated processing temperatures would serve to volatilize

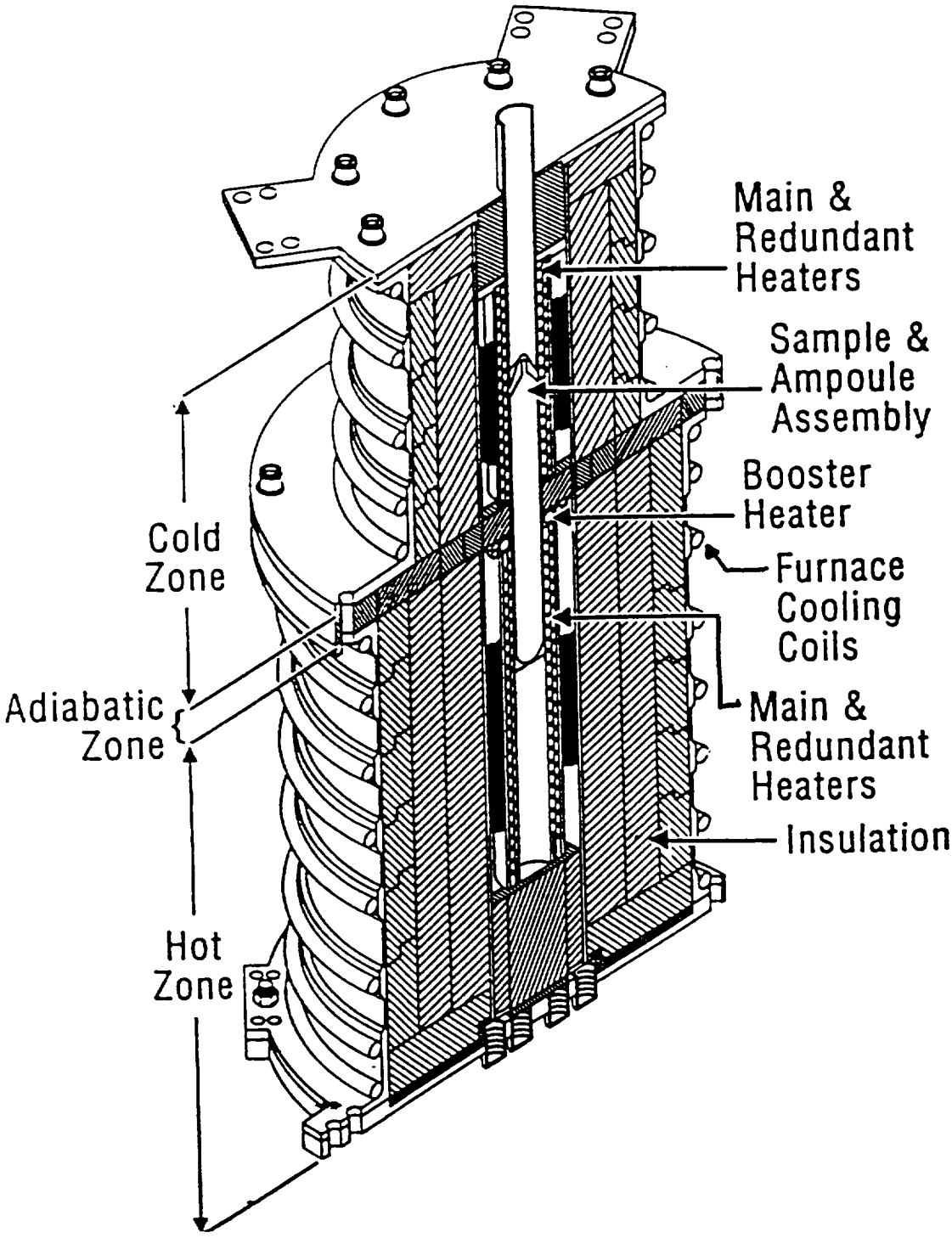


Figure 3: Reconfigurable Furnace Module (RFM)

(NASA/MSFC, SP-DOC-6102, March 1990)

the sample, possibly driving the material out into the EAC if an escape route exists. Second, the current method to detect sample materials in the EAC is by visual inspection of vapor deposition on a reflecting plate. This method cannot distinguish between the deposition of hazardous materials released from the ampoules and benign substances outgassed or condensed from furnace materials.

One factor constraining the use of more elaborate failure detection techniques is the limited space available within the furnace assembly. Most of the volume inside the EAC is filled with the furnace, the translation system, and the SEM. Additionally, the cartridges for the Marshall Space Flight Center (MSFC) version of the experiment are 59.16 cm long, with 16.00 to 28.43 cm of that envelope being occupied by an ampoule, and only 2.5 cm in diameter. Any method of failure detection located within the cartridge would need to be extremely compact and, depending on its location with respect to the ampoule, able to withstand high temperatures. Equally important is that a potential failure detection system not present a safety hazard in itself, and that it not adversely affect the crystallization process.

## 1.3 Objective

The overall objective of this work is to determine possible solutions to the current safety problems resulting from a leakage of the toxic compounds from the CGF. Any method used to accomplish this task must adhere to current NASA safety specifications and regulations, as well as meet the experiment specific criteria detailed in the previous section. Hence, the overall objective is divided into two separate, but related components.

The first objective is to evaluate potential methods for detecting the failure of the containment structures used in the CGF. The second objective is to examine the transport and deposition of sample materials in the event of an ampoule/cartridge failure. This second task will itself be broken into two parts. The first goal is to determine the ultimate fate of sample compounds following a combined ampoule/cartridge failure, and if any conditions exist under which a significant sample vapor concentration could exist within the EAC. The second goal is to use this analysis to estimate the effectiveness of leak detection methods that rely on the direct sensing of sample materials.

## 2.0 LITERATURE REVIEW

The literature survey presented in this section is divided into three portions: quantitative detection methods, qualitative detection methods, and experiment specific documentation. Specifically, quantitative methods directly measure the vapor phase concentration of sample species while qualitative methods rely on some secondary effect, such as deposition onto a substrate, to detect a species. Principles of operation and possible implementation for these methods will be detailed in the next chapter. The third sub-section reviews the NASA documents that define the specific parameters and requirements for the MSFC CGF experiment.

### 2.1 Quantitative Detection Methods

#### 2.1.1 Atomic Absorption Spectroscopy

The presence of most metals can be quantitatively determined through atomic absorption spectroscopy (AAS), a technique that exploits the tendency of elements to absorb radiation at characteristic wavelengths. Rosentreter and Skogerboe (1991) used AAS to detect trace amounts of cyanide in an aqueous solution. Using the reaction between cyanide and silver to produce a

dicyanosilver complex, they were able to detect the presence of cyanide to 0.002 milligrams per liter. The silver, easily detected by flame AAS methods, was introduced to enhance the overall limit of detection.

Alternative methods to flame AAS include electrothermal atomization (ETA) and hydride generation. As described by Hershey and Keliher (1989-90), modern ETA techniques place a sample within a tube and inside a modified furnace before heating. ETA/AAS offers increased sensitivity over flame AAS, with typical detection limits in the parts per billion (ppb) range, but is subject to problems of matrix interferences and molecular absorption. Another approach described by Hershey and Keliher surmounts these problems by converting elements capable of forming volatile hydrides to the hydride, and then separating them from the matrix just prior to AAS determination. Called hydride generation, it has been used to detect antimony, arsenic, bismuth, lead, and tin among others elements. Thermo Jarrell Ash Corporation (1992) reports the AVA880, one of their commercial AAS instruments using hydride generation, allows detection of arsenic and selenium to 0.1 ppb and 0.2 ppb respectively. The AVA880 can also detect mercury to 0.1 ppb using a cold vapor technique which reacts mercury with stannous chloride.

However, all AAS methods require background correction when the sample contains other material capable of absorbing light at the same wavelength as the element in question. Sotera and Khan (1982) conducted a brief comparative study of the two most commonly used correction techniques: Zeeman and Smith-Hieftje correction. A description of these two methods may be found in section 3.1.1.1 of this report. It was found that the Smith-Hieftje method not only had all the advantages also common to Zeeman systems, namely correction in visible as well as ultraviolet spectrum regions and correction of spectral interferences, but it also had many advantages over Zeeman systems. Smith-Hieftje does not constrict either the source or sample areas, may be applied to both flame and furnace AAS, has no loss of light due to polarizers, and is much less expensive. As a point of interest, the AVA880 system mentioned earlier uses Smith-Hieftje correction when conducting a multi-element analysis of a sample.

### 2.1.2 Atomic Emission Spectroscopy

Similar to AAS is atomic emission spectroscopy (AES), which analyzes the characteristic radiation emitted by an excited sample. Van Veen et al. (1992) quantitatively determined the presence of trace elements in uranium using AES methods coupled with Kalman filtering. The filter

allows direct measurement in the matrix by eliminating spectral interferences and should therefore yield detection limits comparable to those for pure component solutions. Yet the results found detection limits worse than the pure solution limits by a factor of one to four. They determined that the inductively coupled plasma (ICP) AAS technique itself and not interference from the uranium limited their sensitivity.

Majidi et al. (1991) used AES with an electrothermal atomizer and laser excitation to determine trace metals in liquid samples. A laser induced plasma approach was chosen to minimize matrix interferences within the sample. Conducting a simultaneous multi-element analysis, they were able to detect cobalt and cadmium in micrograms per liter concentrations.

Their work illustrates the common use of lasers as excitation sources in AES, one such method being a laser generated spark. Often referred to as spark source emission spectroscopy (SSES), it is a research technique that is now commercially available as well. Radziemski et al. (1983) used a repetitive laser pulse as an excitation source in ambient air and coal gassification systems. They were able to provide real-time, in situ analysis that detected both arsenic and mercury to 0.5 parts per million (ppm). An array of photomultiplier tubes (PMT) was used for detection of the emitted radiation, using a signal

averager to provide time resolution. The output resolution was necessary to discriminate against strong continuum emission occurring within the first 500 nanoseconds.

As in the Radzieman experiment, PMTs are the predominant form of detection currently used in AES. Although they provide an instantaneous readout of intensity at each monitored wavelength, detection is limited by the number of PMTs that can be located on the focal plane. Solid-state array detectors, as explained by Fields and Denton (1992), may offer a solution to this limitation. Solid-state array detectors such as the charge-injection device (CID) have hundreds-of-thousands to millions of detector elements in a very small, rectangular format. CIDs combine high resolution with sensitivity, dynamic range, and spectral coverage superior to PMTs. Recently applied to a direct-current arc AES analysis, CID detection in an echelle spectrometer is now commercially available from Thermo Jarrell Ash Corporation. Preliminary results demonstrate detection limits comparable to or better than traditional PMT systems.

Additional information regarding recent advances and techniques in AES may be found in a review compiled by Beauchemin et al. (1992) for *Analytical Chemistry*. The review thoroughly covers sampling techniques, excitation sources, detection systems, and data processing.

### 2.1.3 Mass Spectrometry/Gas Chromatography

A more commonly used technology for quantitatively determining constituents within a vapor sample is mass spectrometry (MS). Comprehensively described by Frigerio (1974), MS techniques separate and record the masses of ionized atoms with typical detection limits in the parts per trillion (ppt) range. Ketar et al. (1991) detected chemical warfare agents in ambient air using tandem quadrupole MS in conjunction with atmospheric pressure ionization. They were able to accomplish real-time detection below 20 ppt for two different nerve agents with a response time of 15 seconds.

Several variations of standard MS techniques have been used for atmospheric analysis as well. Among these, Arnold et al. (1991) attached a vapor transfer line to a combination gas chromatography/mass spectrometry (GC/MS) system. The line, consisting of two fused silica and one glass lined steel columns, connected to the GC/MS such that atmospheric background was minimized when the system was not sampling. It also preserved the ratio of the

constituents during sampling, and successfully monitored transient concentrations of aromatics in the ppb range.

Unfortunately, MS, and especially GC/MS, systems are bulky and rather cumbersome to deploy in field experiments or in constricted areas. Recognizing the need for such instrumentation, Sinha and Gutnikov (1991) designed a comparatively miniaturized GC/MS system. They used a short (50E-6 m inside diameter, 3 m length) microbore capillary column, and were thereby able to use an extremely small gas rate of 0.05 atmospheric $cm^3/min$. This eliminated the need for large pumping equipment, greatly reducing the weight and power requirements for the overall system. An array detector and scaled down version of a focal plane MS assisted in maintaining high sensitivity while minimizing size. While their system was successful, the authors recognized the need for continued development of field-portable units before a satisfactory, truly miniaturized design is created.

### 2.1.4 Electrochemical Sensors

A completely different approach to quantitative vapor-phase determination involves a species-specific electrochemical sensor. The technology is not nearly as well developed as AAS, AES, and MS, but has been used extensively to detect oxygen. The sensor acts as an electrochemical cell, producing a voltage related to the

concentration of the vapor of interest. Weimhöfer and Göpel (1991) report that using different electrolyte materials may reduce the cross sensitivities of the sensors to other reactive gases present in the detection environment. Their theoretical study of surface chemistry at electrolyte/electronic conductor interfaces identified the nature of the problem, and stressed the need for continued, systematic development to design less cross-reactive sensors. Additional investigation of potential electrolyte materials was conducted by Alcock et al. (1991). They successfully extended the temperature and pressure ranges at which oxygen sensors could operate by using composite fluorides and perskovite oxides in place of the zirconia electrolyte typically used.

### 2.1.5 Fiber Optic Sensing

Fiber optics have been used by researchers as chemical gas sensors using numerous methods. In a summary of the principles and problems associated with this approach, Narayanaswamy and Sevilla (1988) elaborate on two types of optical fiber sensors. The first, called spectroscopic sensors, detects species directly through their characteristic spectral properties. In this case, the fiber functions only as a light guide, conveying the light back and forth from the source to the detector. The second type of sensor uses a chemical transduction method

which alters some optical property through interaction with the species of interest, hence the term chemical sensors.

In this latter category, Blyler et al. (1989) incorporated a dye in plastic-clad, fused-silica (PCS) optical fibers. Small chemical species rapidly diffuse through the silicone, changing the absorption loss characteristics of the fiber as they react with the dye. Using a pH-sensitive dye, the authors succeeded in measuring the concentration of ammonia with a maximum time delay of 25 seconds. They also used a fluorescent dye to detect oxygen concentrations in an oxygen/nitrogen atmosphere.

In addition to the methods mentioned above, Moslehi et al. (1992) review many other fiber optic detection techniques. Among these are interferometric sensors, which have been used to detect as little as 20 ppb of hydrogen in one atmosphere of nitrogen. The sensor consists of a paladium-coated optical fiber. The coating enhances hydride formation, causing the fiber core to expand and contract as the hydride lattice grows and shrinks. Hydrogen concentration is determined by monitoring the optical interference in reference to an uncoated fiber.

Another method reviewed by Moslehi et al. is similar to the dye-doped fibers mentioned above. Tapers of hollow

metallic beam expanders/concentrators are created using electroforming techniques to optimize their signal-to-noise ratio and bi-directional sensitivity. A chemical dye cell covered by a membrane is then incorporated in the expander/contractor. Gas that permeates through the membrane mixes with the dye and is excited by the incident light. This excited mixture emits fluorescent light at a different wavelength, the intensity of which is directly proportional to the concentration of the gas. Arrays of these sensors may be banded together, for multi-gas or multi-parameter sensing. At present, however, none of these methods are commercially available.

## 2.2 Qualitative Detection Methods

### 2.2.1 Ultrasonic Testing

Ultrasonic techniques have been one of the most widely used forms of non-destructively testing a structure to locate flaws. Szilard (1982) edited a comprehensive collection of reviews on ultrasonic testing principles and methods, but it concentrated on the use of transducers as the primary means of generating ultrasonic waves. Predominately piezoelectric, these transducers have several drawbacks including limited operation on irregularly shaped objects and mandatory contact with the specimen. Sarrafzadeh et al. (1988) used a laser generated technique, and were able to identify surface

defects on a railroad beam. Using a pulsating laser as the excitation source, they avoided the problems associated with piezoelectric devices, but noted that the method still required much development.

### 2.2.2 Make-Wire Sensor

Johnson and Galloway (1990) developed and tested a prototype sensor that responds to metallic deposition with a decrease in resistance. Essentially an electrical circuit with small breaks in the wire, closure of the breaks by a depositing metal species results in a resistance attenuation from infinity to some lower value. Preliminary testing conducted at MSFC was successful for all of the crystal growth materials tested, but further research is needed to determine the sensor's potential in a crystal growth environment under flight conditions.

### 2.2.3 Pressure Gauges: Piezoelectric and Piezoresistive Transducers

Pressure transducers, in the form of piezoelectric and piezoresistive devices, are the most standard form of pressure measurement currently used in industrial and commercial applications. A broad review of piezo-instrumentation theory and applications is given in a catalogue published by Kistler Corporation (1989), in addition to listings and specifications concerning their

available models. Uses range from high pressure ballistics to low level hydraulic measurements and engine monitoring in rockets. For static measurements, the type needed if applied to the CGF environment, piezoresistive devices offer the best response. One such Kistler model, the 4045A, is described in their *Piezoresistive Measuring Instruments* catalogue (1992). It measures with respect to absolute pressure and operates up to 120 °C while maintaining linearity and hysteresis to 0.3% full scale and 0.1% full scale respectively. The unit has dimensions of 45 mm in length and 16 mm in width.

More recent developments in piezoresistive technology have led to solid-state sensors micromachined from silicon. Hall (1991) reports that silicon sensor chips have greater sensitivity and resiliency than standard piezoresistive devices, and have operated successfully at temperatures up to 260 °C. The approach uses silicon as the basic substrate with an insulating layer of silicon dioxide providing dielectric isolation.

### 2.2.4 Fiber Optic Pressure Sensors

One of the more recent developments in remote pressure sensing involves the use of optical fibers in conjunction with a pressure sensitive diaphragm. Murphy and Jones (1993), noting the widespread confidence in

standard pressure gauge technology, described a system which does not entirely replace the transducer unit, but instead retro-fits an optical alternative to a conventional diaphragm. The authors bonded an optical strain gauge to the center of a ceramic diaphragm, and measured the optical retardation through optical fibers as the diaphragm deformed with changes in pressure. Murphy and Jones obtained a resolution of 0.3 kPa, but did not achieve the anticipated linear response. The authors asserted that the clamping arrangement may have induced sufficient pre-strain in the gauge to cause the errors.

Another technique, used by Henderson et al. (1993), monitors the chromatic transmission resulting from a deflecting diaphragm between a pair of optical fibers. They constructed a sensor of this type for use in the 0 to 400 kPa absolute pressure range, and were able to maintain a resolution of 150 Pa during short term testing. The system was designed for remote pressure monitoring of an explosive reaction vessel, using a fiber length of 300 m. With such an expanse for the transmissions to traverse, changes in the source emission and bending of the fibers adversely affected the testing over longer time periods.

However, yet another method of fiber optic pressure sensing has been used and, being more reliable than the two forementioned techniques, is now commercially available. A reflective diaphragm on the end of the

sensor flexes inward with increasing pressure, thus modulating the color of the reflected light. The variation in color is then translated into a pressure measurement by the supporting instrumentation. A division of Metricor, Phonetics Inc. (1993), supplies both metallic and non-conductive versions of the sensor, both maintaining a resolution of 0.7 kPa (0.1 psia) for a measurement range of 0 to 1000 kPa (150 psia).

### 2.2.5 Microbalances

Advances in piezoelectrics have led to one of the more rapidly developing fields of in situ mass detection. Ward and Buttry (1990) report that piezoelectric technology in the form of microbalances has been used to dynamically measure minute mass changes at less than one nanogram per square centimeter. The most common of these devices, the quartz crystal microbalance (QCM), has been used to detect pollutants such as sulfur dioxide and mercury by treating the transducer with a coating that increases in mass as it reacts with a specific analyte. Ward and Buttry also report that another QCM method, pattern recognition, has discriminated among different hydrocarbons and alcoholic beverages with success rates around 80%.

A different approach to QCM technology was used by Zakipour and Leygraf (1986) to study corrosion kinetics on

electrical contact materials. They used an array of nine oscillating quartz crystals, each having a 9 mm diameter and 0.2 mm thickness, coated on each side with a 5 mm gold layer 500 Å thick. Monitoring the crystals simultaneously with a computerized data acquisition unit, a mass resolution of less than 1E-8 g/cm$^2$ allowed them to study the initial stages of atmospheric corrosion by sulfur dioxide and nitrogen dioxide.

As the use of microbalances in electrochemical studies is becoming more common, Gabrielli et al. (1991) attempted a calibration of a QCM under those conditions. They studied both homogeneous and localized changes in mass on the electrode surfaces, experimentally determining the average and differential sensitivities. Although their efforts were successful, the authors concluded that the electrochemical QCM must be calibrated according to the experimental conditions governing each particular case.

### 2.2.6 Perfluorocarbon Tracers

Conservative gaseous tracer technology originated from the need to study atmospheric pollution without introducing additional contaminants into the ambient surroundings. Conservative tracers are defined as those which react neither chemically or physically in any way with the environment. Dietz and Senum (1984) assesed the

needs and capabilities of this family of tracers, concluding that perfluorocarbon tracers (PFT) held the most promise for future use. PFTs were found to have extremely low ambient background levels, non-existent toxicity, non-reactiveness, and be easily detected by standard GC methods.

In the years since their discovery for use as tracers, PFTs have developed a symbiotic relationship with the instrumentation designed to detect them. As better instruments were constructed, PFT use and research increased, thus the instruments were refined, and so on. One such example described by Dietz (1986) is the Brookhaven Atmospheric Tracer Sampler (BATS). Developed by Dietz at Brookhaven National Laboratories (BNL) under contract to the National Oceanographic and Atmospheric Association (NOAA), BATS has distinct advantages over its predecessor which sampled by passive capillary adsorption. BATS is programmable, thus able to sample at different rates, and offers better sensitivity and time resolution than the earlier technique. However, for final analysis of PFT concentrations, the BATS must still be taken back to the laboratory and connected to an electron capture device/gas chromatography (ECD-GC) system.

These limitations led to the refinement of the Dual-Trap Analyzer (DTA), originally developed by J. Lovecock in 1977 for NOAA, by BNL researchers. D'Ottavio et al.

(1986) report using a DTA for real-time analysis during several PFT experiments. The DTA has a built-in ECD-GC, and although it has an hundred-fold less resolving power than the laboratory system, it has successfully separated three PFTs in a four minute sample with an approximate detection limit of 5 to 10 femtoliters (1 femtoliter = 1E-15 liter).

In a more recent application, Dietz and Goodrich (1991) demonstrated the technology's usefulness for rapid, sensitive leak certification of SSF modules. In a test conducted at MSFC in 1991, Dietz and Goodrich quantified leak rates on a surrogate module. The rates, unknown to Dietz and Goodrich, were pre-set by MSFC scientists who also observed the testing. Having never performed this type of analysis before, a few mistakes in the testing procedure were made by the BNL team, but were readily identified in their final report. The authors did successfully demonstrate that leaks as small as one milliliter per minute could be detected in real-time using a DTA system. After subsequent analysis of the results, the authors asserted that overall precision of 10% to 15% was attainable using real-time instruments.

In more commercial applications, Dietz (1991) reports that PFT technology has been used to detect and locate leaks in underground cable systems and storage tanks. Also used for hermicity testing of electrical components,

a DTA has quantified leaks from 0.2E-8 to 1.0E-3 ml/s in just twelve minutes. Potential uses under investigation include pre-fire detection and integrity testing of food packaging.

### 2.2.7 Radiotracers

Other techniques used in leak detection rely on radioisotopes as tracers. A comprehensive review of the theory and selection of radiotracers was edited by Foldiak (1986), and includes industrial applications. Typical uses in the area of leak detection include monitoring pressurized power cables, gas filled telephone cables, and other relatively low-volume systems. Use in larger systems such as gas pipe lines is precluded by safety issues resulting from the possible escape of significant quantities of radioactive gas into the atmosphere.

Kleinknecht (1986) examined numerous radiation detection devices, including those based on the measurement of ionization, particle identification, and time. The author comprehensively described the principles behind their operation and gave examples of various applications associated with different systems. From this account, gas filled detectors and scintillation counters appear best suited for CGF application and will be discussed further in section 3.2.2.2 of this report.

### 2.2.8 Surface Reflectance

Fiber optic reflectivity sensors have been used extensively by researchers to indicate the presence of various contaminants. In one such experiment, Butler et al. (1990) used micromirrors deposited on the end of optical fibers to detect various volatile organic compounds. The reflectivity travelling back down the fiber is dependent on the thickness of the mirror layer, which changes as the compounds deposit out. For their experiment, the authors used a 50 Å thick semi-transparent chromium mirror and a deposition rate of 8 angstroms per second. Hughes et al. (1991) report that the micromirror sensors have been used to detect other species as well. So far, the method has also successfully detected mercury, oxygen, nitrogen dioxide, hydrogen sulphide, and sulphur dioxide. The mirror material is chosen to react with the chosen contaminant, thus changing the reflectivity through chemisorption.

## 2.3 Experiment Specific Documentation

Several NASA documents were reviewed to obtain specific information on the CGF facility and requirements governing its operation. They include the following: parameters for each of the four crystal growth experiments flown on USML-1 were found in NASA/MSFC documents ICD-2-60026 through ICD-2-60029 (1990); a detailed system

design description was given in NASA/TBE SP-DOC-6102 (1990); safety requirements concerning the release of hazardous chemicals were listed in NASA/JSC NSTS-1700.7B (1989); and data used to determine temperature profiles within the cartridge was found in NASA/TBE SP-RPT-6752 (1991) and TBE memorandum MEPF-CGF 2/93-311 (1993). Since CGF materials and processing requirements are likely to be similar on future flights, the information contained in these documents was used as the basis for the analyses contained in this report. A summary of sample materials and processing conditions for the CGF experiment flown on United States Microgravity Laboratory 1 (USML-1), the data on which the analyses of this project have been based, is given in Appendix B of this report. Additionally, Appendix D summarizes possible biological effects from exposure to common crystal growth materials.

A comprehensive review on the preparation of solid state materials and the dependence of the material properties on preparative conditions was edited by Wilcox (1976). Further data regarding the volatile species and their vapor pressures was found in the NASA documents listed above and *The Handbook of Chemistry and Physics* (1992-1993). Relations for the Fanno flow analysis discussed in section 4.2 were adapted from Shapiro (1953), and Miller (1983).

## 3.0 FAILURE DETECTION METHOD DESCRIPTIONS

The detection methods described in this section will be divided into three categories: ampoule leak detection methods, cartridge leak detection methods, and methods which detect species within the EAC. As in the literature review, the ampoule leak detection methods will be separated into quantitative and qualitative groupings. Cartridge leak detection methods, all being qualitative in nature, will be divided according to the principle means of detection: a change in pressure or a gaseous tracer. Finally, the two detection methods for the EAC, mass spectrometry and spark source emission spectroscopy, will each be detailed in separate subsections.

### 3.1 Ampoule Leak Detection Methods

#### 3.1.1 Quantitative Methods

##### 3.1.1.1 Atomic Absorption Spectroscopy

The vapor-phases of the metallic species used in crystal growth experiments absorb and emit radiation at discrete visible and ultraviolet wavelengths characteristic to each element. Atomic absorption spectroscopy (AAS), which measures the absorption of

radiation by free atoms, exploits these narrow, elemental line absorption characteristics to identify specific constituents within a vapor. In AAS, a very narrow band source of radiation corresponding to a designated absorption line is projected through the volume containing the species vapor, and a monochromator tuned to the wavelength of the source measures the decrease in radiation. The amount of light absorbed by the sample is a function of the number of absorbing atoms in the path.

The source of radiation is usually provided by a hollow cathode lamp. The lamp is filled with an inert gas, typically neon, which is ionized by the anode. The ions are then attracted to the cathode and, if possessing sufficient energy, the collision causes the atoms of the cathode to be ejected. These sputtered atoms are excited and emit radiation characteristic to the cathode metal. Since atoms only absorb at their own characteristic wavelength, a hollow cathode made from the same element allows a high degree of freedom from interference by other elements. Unfortunately, this also means that a separate light source must be used for each element to be detected.

When a sample contains some other material that can absorb light at the element wavelength, background correction must be used. This background absorption is primarily caused by molecular absorption and particle scattering. In commercial AAS applications, it is

corrected for by using the Zeeman effect or by varying the current in the hollow cathode lamp, commonly called Smith-Hieftje correction. Briefly, the Zeeman method uses a strong magnet to split the absorbed or spectral line into three components: a central line of the original wavelength, and two sidebands of equal magnitude that are shifted in wavelength. Subtraction of the sideband signal from the central signal provides the Zeeman correction. The Smith-Hieftje method passes an excessive current through a hollow cathode lamp, broadening its emission line and thus reducing the sample absorbance. Since the background will absorb the same proportion of light as before, correction is obtained by taking the difference in the two signals.

Even using background correction, it appears the resolution of AAS would not achieve the parts per million detection standard required in the cartridge environment. The instrumentation requirements present an additional obstacle. It would be possible to mount the hollow cathode lamps and monochromators in the EAC, and use fiber optics to transmit radiation into and out of the cartridge. However, considerable development would be necessary to construct lamps and detection systems that do not have excessive power and/or voltage requirements and are flight certifiable.

### 3.1.1.2 Spark Source Emission Spectroscopy

Similar to AAS is plasma emission spectroscopy, which uses the line emission characteristics of elements to identify their presence within a vapor. Emission is frequently induced through a continuous, high-voltage arc or an intermittent, high-voltage spark. Generating the plasma with the spark source, the duration of which is less than one millisecond, reduces power consumption. This approach is refered to as spark source emission spectroscopy (SSES), and is capable of measuring concentrations of all the metallic constituents within the plasma simultaneously. In principle, the sample atoms are ionized by the spark and emit narrow lines of radiation as they return to the ground state. A diffraction grating is typically used to resolve the emission lines into their spectral components while an array of radiation detectors measures the intensity of each line of interest.

SSES, which has accurately determined trace concentrations in the parts per billion range, offers a significantly improved detection limit over AAS. Another advantage is the reduced instrumentation required for implementation of SSES, mainly from the elimination of the hollow cathode lamps. Even so, adaptation of SSES for use inside the cartridge environment would require a substantial effort. Fiber optics could be used to transmit the emitted radiation out of the cartridge, but

the spark source itself would still need to be located inside the cartridge. Generating such a high-voltage spark inside the cartridge could result in electromagnetic interference with the crystal growth process. While this method does not seem to lend itself for safe use within the cartridge, it does present itself as a possibility for contamination monitoring of the EAC environment and will be discussed further in section 3.3.2 of this report.

#### 3.1.1.3 Electrochemical Sensor

An alternative approach to quantitative species detection uses an electrochemical sensor. Well-established in analytical chemistry, the sensor is an electrochemical cell designed to detect a specific gaseous species. The cell is constructed using a material or materials which will undergo a reversible chemical reaction with the vapor species of interest and produce a voltage related to the concentration of the vapor-phase species. The electromotive force (EMF) across the electrolyte is given by the Nernst equation. Using a classical oxygen concentration cell as an example, the equation would be as follows:

$$E=\frac{RT}{nF}\times\ln\frac{p'}{p''}$$

where R is the gas constant, T is the temperature, F is Faraday's constant, n is the number of electrons in the reaction (determined empirically), and p' and p" are the partial pressures of oxygen at the two electrode/ electrolyte interfaces. Thus if p' is kept contant at the reference electrode, the voltage at constant temperature is directly releated to p". Controlling the reactions and their equilibria at the electrode interfaces is the key to designing reliable sensors.

Although electrochemical sensors have been used extensively to quantitatively detect oxygen, developing sensors for the sample species used in crystal growth would require a sizable effort. Since each cell is species-specific, suitable solid-phase materials and their reactions with a species would need to be identified for each toxin. This development would essentially be undertaken from scratch, and issues such as compatibility with SACA materials and operational reliability would still need to be addressed. Given the technology's immaturity, it is unlikely to be adequately developed for use on near-future flights.

### 3.1.2 Qualitative Methods

#### 3.1.2.1 Make-Wire Sensor

Metallic species that escape from a broken ampoule will deposit onto surfaces that are at a temperature lower

than the dew-point temperature of the vapor. The make-wire (MW) sensor, developed and tested at MSFC, uses this deposition to close an electrical circuit. The sensor is constructed from a 0.1 mm diameter iron wire wound helically around an alumina support with a 1.0 mm break in the wire. A new version of the sensor under development is to be constructed from an alumel thin-film on a quartz substrate measuring 2.54 mm long, 1.71 mm wide, and 0.25 mm thick with many parallel open circuit alumel trails. In principle, a small gap in the sensor is closed by the deposition of sample vapor, thus decreasing the resistance in the circuit from infinity to some lower value. Although initial testing has been successful in demonstrating the feasibility of the method, several issues still need to be addressed.

First, preliminary testing has been conducted in controlled furnace environments. It needs to be determined if outgassing of other materials in the SACA will deposit onto the sensor and produce a positive detection. Additionally, reliable operation of the MW sensor requires that sufficient metallic deposition occur very close to the gap, forming an adherent film on the electrical contacts of the circuit. This is highly dependent on the temperature of the sensor and the mass transfer processes occurring within the cartridge. An accurate prediction of sample vapor transport and

deposition under microgravity conditions is needed to assess the viability of the MW sensor under flight conditions.

#### 3.1.2.2 Surface Reflectance

An alternative method to detect the deposition of a sample species monitors the reflectance of a surface exposed to the condensing vapor. A relatively simple reflectance sensor could be constructed using a fiber optic coupled with a diode or LED laser and a photovoltaic detector to sense radiation. Visible or infrared radiation would be transmitted into and out of the cartridge through the fiber optic, the terminating end of which would serve as the deposition surface. Deposition of metallic species onto the end of the fiber would alter the back-reflection of the optic.

The advanced level of fiber optic technology would not make it difficult or expensive to construct such a sensor. However, like the MW sensor, a reflectance sensor would be highly dependent on vapor transport and deposition processes within the cartridge for reliable operation. The same possibility of falsely detecting a leak due to the outgassing of harmless materials within the SACA also exists. Extensive experimental testing would therefore be necessary to accurately assess the performance of a reflectance sensor.

Other research in this area has developed species-specific reflectivity sensors. Reflectivity changes have been measured using optically thin silver films evaporated onto the end of an optical fiber to detect various molecular species such as hydrogen sulfide, nitrogen dioxide, and chlorine gas. Additional experiments have successfully monitored mercury using a gold film, and hydrogen gas using palladium. The gaseous species react with the metallic films to alter the back-reflection in the optic. Unfortunately, no species-specific reflectivity sensors are currently commercially available, and research of film materials to detect other species is far from complete.

#### 3.1.2.3 Ultrasonic Detection

Unlike other methods which detect an ampoule failure from an escaped species, an ultrasonic technique would directly assess the integrity of the ampoule itself. Routinely used to detect flaws in pipes, ultrasonic testing may be used to non-destructively detect small cracks in the ampoule surface. The most common form of ultrasonic testing, the pulse-echo technique, uses separate transducers on opposite sides of a potential crack to serve as transmitter and receiver. The presence of a crack will either partially or completely interrupt the pulse transmission, depending on the depth of the

crack relative to the depth of wave penetration. The amplitude of the received signal may then be used to estimate the crack depth.

Frequency ranges of the transmitted signals are typically on the order of a few megahertz. A major concern is that sending such a pulse through the ampoule could have adverse effects on the crystallization process, inducing defects within the crystals. An additional disadvantage of this method is that most ultrasonic transducers are piezoelectric and depolarize at high temperatures. Of the commonly used piezoelectric materials, quartz has the highest depolarization temperature at 575 °C. Experiments on the CGF usually range from 350 °C to 1260 °C, precluding the use of piezoelectric transducers very near the ampoule. Other possible excitation sources, such as pulsating lasers, have been successfully used in research. However, this is not yet a commercially available option, and locating a laser inside the cartridge to generate ultrasonic waves through the ampoule is not a logical alternative.

#### 3.1.2.4 Microbalances

Microbalances have been used for years in surface chemistry to monitor mass deposition in microgram amounts. A number of variations have been developed, which can generally be classified as either "classical" or quartz-

crystal microbalance (QCM) types. The classical instruments measure the change in load created by a change in mass, thus requiring a stable gravitational field and making them unsuitable for use in space. This leads to the more recently developed piezoelectric quartz crystal microbalance (QCM), used extensively as a thickness monitor for thin solid films, which does not rely on the presence of gravity for its measurements. The QCM oscillates at a resonant frequency which is easily affected by a change in mass, even in a weightless environment.

A QCM is constructed from a very thin wafer of piezoelectric material sliced from a single crystal. Two electrodes are then attached to the wafer and connected to a periodic voltage source which is used to induce an oscillating electric field. This field is generated perpendicular to the surface of the wafer, thus producing a mechanical oscillation. The resonant oscillation is obtained by connecting the wafer to a circuit specifically designed to oscillate at the wafer's fundamental frequency. This makes the microbalance highly sensitive to any mass deposited on its surface since the resonant frequency is dependent on the total mass of the vibrating body.

In principle, any piezoelectric material could be used, but quartz is chemically stable, low in cost,

readily available, and a high frequency resonator. Its tendency to resonate at high frequencies decreases its sensitivity to fluctuating temperatures and pressures. This is a very desirable quality since the resonant frequency change due to these effects needs to be small when compared to a change in mass for measurement accuracy. Another factor affecting the performance of the QCM is the specific crystallographic orientation at which the wafer is cut. The oscillating wafer vibrates primarily in the shear mode, and the two major surfaces need to be antinodal. The orientation of the cut can also be used to reduce sensitivity to temperature variations.

QCMs can detect mass deposition of only a few atomic layers, corresponding to sub-microgram levels, in controlled environments. Since this type of microbalance is sensitive to the mass change per unit area, miniaturization of the device does not sacrifice its accuracy. Any small amount of mass deposited on the surface of the wafer will result in a decrease in the resonant frequency.

As with any ultrasensitive measuring device, it needs to be established that the balance is actually detecting the species in question and not responding to fluctuations in temperature and pressure or deposition of non-threatening substances. One limitation of QCMs is that they can not be subjected to temperatures in excess of

approximately 450 °C without the piezoelectric crystal beginning to depolarize. This would necessitate placing the microbalance at the top of the cartridge close to the SEM cap. However, any species migrating from a failed ampoule might not reach this location. A contaminant could diffuse in that direction, but deposit on the various substances currently packing the cartridge before reaching the detector. Additionally, the QCM would also detect any deposition from outgassing of harmless materials located within the cartridge without the ability to determine if they were indeed harmless, or if the ampoule had failed.

## 3.2 Cartridge Leak Detection Methods

### 3.2.1 Pressure Measurement

#### 3.2.1.1 Pressure Gauges: Piezoelectric and Piezoresistive Transducers

Piezoelectric transducers are used for a wide variety of applications including force, pressure, and acceleration measurements. Not used commercially until the 1950's, the devices utilize the tendency of certain crystals to produce an electrical charge when subjected to mechanical loading. Although several different crystal

species exhibit this property, most commercially available transducers use quartz as the crystalline sensing element.

Two of the most important properties of quartz include its high linearity and negligible hysteresis effects. Equally crucial, however, is the relatively constant sensitivity quartz maintains over wide temperature ranges. Along with its low cost, availability, and chemical stability, these properties make quartz ideally suited for this type of application. Some of these qualities may be enhanced by cutting a thin slice of quartz at a specific crystallographic orientation. For example, a shear cut is used primarily in multi-component force transducers, a transverse cut is used for pressure applications, and the Kistler-patented Polystable cut is employed for high-temperature pressure measurements.

In addition to the sensing element, a piezoelectric transducer consists of a diaphragm for transmitting the pressure to the element, and a transducer housing. A certain combination of these three main components will enable a user to tailor the device for a particular pressure range and application. Unfortunately, the diaphragm, usually made of welded sheet metal, will expand and contract with temperature fluctuations. Thus, while the element itself is temperature insensitive, it will respond to the change in load produced by the diaphragm

when the temperature changes. This effect may be reduced through the use of special insulating materials or watercooling around the diaphragm.

Since a transducer will produce an electrical output only when the load changes, it is not capable of performing true static measurements. However, with the proper signal conditioners and insulating materials around the cables and connectors, limited quasistatic capability may be achieved. Using insulating material will serve to lengthen the time constant, or discharge time of the alternating current (AC) circuit. A longer time constant will result in better low frequency response, and therefore, longer useable measuring time.

An additional factor affecting the performance of the transducer is the impedance. Low impedance systems contain a built in charge-to-voltage converter, and are used primarily in well-defined environments. Conversely, high impedance transducers are more versatile. With no built-in electronics, they can operate across a wider temperature range. High impedance units also have longer time constants, thus allowing easier short term static calibration. However, both are AC coupled systems with limited quasistatic capabilities.

Piezoresistive transducers, also called solid-state pressure sensors, are a recent adaptation of the piezoelectric devices. Very insensitive to acceleration

and shock, they offer a true direct current (DC) response and can measure rapid pressure transients. The sensors use a monocrystalline silicon chip as the diaphragm, with a Wheatstone bridge circuit diffused into its surface. Pressure is then converted to an electrical signal through the elastic deformation of the diaphragm. The circuit, composed of semiconductor resistors, will unbalance proportionally to the applied pressure.

Since most environments the sensor is exposed to will contain some type of corrosive medium, the silicon chip needs to be isolated. This is usually accomplished by placing a very thin stainless steel diaphragm over the silicon and filling the gap between them with oil. The type of oil chosen depends on the temperature range to which the device will be exposed, but the oil volume is always kept as small as possible, typically less than 0.1 $cm^3$, in order to minimize thermal effects. Often, the maximum temperature the sensor can withstand is dependent on the operating temperature of the oil and not the silicon chip itself.

The diaphragm is typically exposed to the ambient pressure on only one side. The cavity on the opposing side, sealed hermetically, is either evacuated or ventilated depending on whether absolute or differential measurement is desired. However, most differential applications are reserved for static, high pressure environments.

Unlike piezoelectric devices, these transducers need to be supplied with a constant current excitation. A signal is not generated unless the Wheatstone bridge is powered. Very low currents, on the order of 1.0 milliamp, will usually suffice. However, since the output is also proportional to excitation current, the current supply needs to be regulated and constant.

As mentioned previously, these sensors are highly sensitive and react quickly to small fluctuations in pressure. Unfortunately, sensors this sensitive will also react to relatively minor temperature changes. This residual temperature dependence can be compensated for by electrically isolating the sensing resistors. For instance, adding parallel and series resistors to the individual bridge arms will linearize the sensor's response to temperature.

For applications within the CGF, a piezoresistive transducer would be more sensitive to the minor changes in pressure that need to be detected. Unfortunately, this

type of transducer requires a constant supply current and is sensitive to temperature fluctuations. Even the models specifically constructed for use in high temperature applications cannot withstand temperatures in excess of 500 °C. Also, as the temperature increases, the pressure exerted by the argon in the cartridge will increase (even without a cartridge failure). To accommodate this, the transducer would need to be connected to supporting electronics that allowed a given range of pressure before sending a positive signal.

#### 3.2.1.2 Fiber Optic Pressure Sensors

Fiber optic pressure sensors have several advantages over their piezo-based counterparts. First, they are electrically isolated and therefore immune to electromagnetic or radio interference. They can also be used in hazardous environments containing corrosive or explosive chemicals. The sensor probe consists of a reflective diaphragm over a shallow cavity. The diaphragm flexes with changes in pressure, varying the color of the light reflected back down the optic. The sensor then converts this color modulation to a measured pressure.

A commercially available sensor operating on this principle, supplied by Photonetics Incorporated, is available with either a metallic or a non-conductive probe. Both have a sensitivity of 0.7 kiloPascals (0.1

psia) for range of 0 to 1000 kiloPascals (0-150 psia), and operate to 200 or 300 °C depending on the specific model. Response time is less than one millisecond. Another advantage of the sensors is their compact size. Probe diameter and length range from 0.8 to 3.2 mm and 10 to 152 mm respectively. Photonetics also supplies the supporting system for the sensors. The instrument is capable of monitoring up to four sensors simultaneously, each with the same or different parameters, and also provides high/low alarms for each channel. The multisensor system has dimensions of 88.9 mm, 368.3 mm, and 431.8 mm for height, width, and depth respectively.

With their small size, the fiber optic sensors could easily be deployed inside each cartridge, and unlike piezoresistive transducers, the fiber optics would not need to be securely mounted. Additionally, the nature of fiber optic technology makes it easy to locate the supporting instrumentation either inside or outside of the EAC.

### 3.2.2 Detection of Gaseous Tracers

#### 3.2.2.1 Perfluorocarbon Tracer Detection

Gaseous compounds are frequently used to detect leaks in a wide variety of applications. One approach involves introducing a tracer gas to a system while using various air sampling techniques to quantitatively detect its

presence external to the system. Brookhaven National Laboratories has conducted numerous experiments in this area using perfluorocarbon tracers (PFTs). The low ambient background levels and low solubility in water of PFTs contribute to their detectability in sub-parts-per-trillion concentrations.

Other advantages of PFTs include their tendencies to be biologically inactive and chemically inert. This prevents the introduction of a leak detection technique into the CGF system that could be potentially harmful in itself. It also eliminates concern about reactions with other materials such that the tracer is neutralized or forms a different toxic substance. Unfortunately, PFTs that have been used in tracer research thus far are viable only up to 500 °C.

Air sampling devices used to detect tracer species use the principles of gas chromatography and electron capture. One such instrument, the dual-trap analyzer (DTA), has the advantages of real-time resolution, in-situ analysis, and high sensitivity all within a portable unit. The air sample is collected using a solid adsorbent, thermally desorbed, and injected into a gas chromatograph which physically separates the sample into its constituents. These constituents are then passed through a palladium catalyst bed to destroy most interfering compounds before proceeding to an electron capture device.

When tracer molecules enter the electron capture device, they interfere with the device's ability to collect the electrons, thereby reducing the current. This reduction in current is used to measure the PFT concentration.

This method has several advantages in that it does not require any power leads or other wiring inside the cartridge, will not disturb the crystal species being processed, uses negligible space inside the cartridge, and is also extremely sensitive. However, although the potential exists to detect very small cartridge leaks, the method will not distinguish which cartridge has failed. A possible remedy to this would be to employ a different tracer species inside each cartridge. Unfortunately, this would necessitate using a single DTA to simultaneously analyze for each of the species. A DTA can currently analyze up to four different tracers (there are six cartridges) and has a minimum cycling time of two minutes. This two minute delay could result in the opening of the EAC after a cartridge has leaked, but before it has been detected. Additionally, the search for a tracer species that is relatively non-reactive and stable up to 1400 °C has thus far produced no acceptable candidates.

### 3.2.2.2 Radiotracers

Use of radioisotopes as tracers is very similar to the PFT method described in the previous section. The radiotracer is deployed in a sealed environment, and its presence outside that environment indicates leakage in the system. The main differences between the two techniques are the methods of detection and possible hazards associated with radioactivity. Using this approach, it is critical to choose an appropriate tracer, and a detection system compatible with the specific type of radiation produced by that tracer.

Radioactivity falls into three basic categories: alpha, beta, and gamma radiation. Alpha radiation is primarily emitted from decay of the heavy elements (atomic number greater than 82), and consists of charged helium atoms. However, it is difficult to measure and the sources of alpha radiation are often extremely toxic, limiting its use as a tracer.

In contrast, beta radiation is much safer and efficiently detected. It consists of electrons emitted from the nuclei of atoms, resulting from neutrons in the nucleus changing into protons. A small thickness of solid material will usually shield a beta emitter, making them useful as tracers in relatively small systems.

Gamma radiation is much more penetrating. It consists of high-energy photons, and is therefore more

useful when the radiation must travel considerable distances through material before reaching the detector. These qualities have led to its use in large-scale studies such as flow measurement in underground pipes.

In addition to choosing the type of emitter for a given application, there are other radiotracer characteristics to be considered. First, the tracer must have a high enough specific activity to overcome dilution in the volume of the system in which it is introduced. Specific activity is a measure of the concentration of the radioactive decay occurring per unit mass or volume in the tracer. In other words, the tracer must be potent enough to release detectable levels of radiation when deployed in a container.

Of equally important consideration is the half-life, or decay rate, of the tracer. The half-life must be long enough to last the duration of the study, so that enough of the tracer is left after that period of time to be detected. It is also beneficial to minimize the amount of radiation persisting after the study, by choosing a half-life of relatively short duration.

In light of these factors, it appears that only beta emitters would be suitable for deployment in a cartridge. The thin cartridge walls will not effectively contain the gamma radiation, and the alpha radiation sources have safety problems of their own. The tracer must also be

chemically inert and a gas. Potential beta radiotracers for cartridge application are given in Table 3.2.

| isotope | half-life(years) | energy(Mev) |
|---|---|---|
| $H^3$ | 12.26 | 0.019 |
| $C^{14}$ | 5730 | 0.156 |
| $Ar^{39}$ | 269 | 0.565 |

Table 3.2: Potential Beta Radiotracers for Leak Detection (Foldiak,1986)

The $C^{14}$ isotope listed above could be used in CO or $CO_2$ to tag the molecule as a tracer, by replacing $C^{12}$.

Detectors for particle radiation convert the incident radiation into an electrical current. They can operate in either the current mode, where the current emanating from the detector is proportional to the rate of radiative interactions with the detector, or the pulse mode, in which each interaction generates an individual electrical pulse. In this case, the rate of interactions is determined by counting the pulses over time. Detector efficiency is defined as the ratio of recorded pulses to the number of quanta incident on the detector. Alpha and beta radiation detectors have efficiencies approaching 100%. However, gamma detectors, which must rely on

secondary effects, have somewhat lower efficiencies. Another detector characteristic is the minimum amount of time which must separate two interactions in order for them to be recorded as two separate events, called dead time. If the dead time is too long and the incidence rate is high, it can result in underestimation of radioactivity levels.

The two types of radiation detectors that appear best suited for use in the CGF are gas filled detectors and scintillation counters. Gas filled detectors operate by collecting the charges created when passage of a radioactive particle ionizes a gas. This category includes proportional counters and Geiger-Muller counters, which operate through a process known as gas multiplication. In proportional counters, the electrons formed by the primary ionization enter a high-voltage electrical field, thus gaining enough kinetic energy between collisions to ionize other gas atoms. As the secondary ionization processes continue, they lead to an avalanche of free electrons. The resulting pulse is proportional to the charge from the primary ionization. Geiger-Muller counters operate using the same principles, but further increase the strength of the electrical field. Due to non-linear effects, Geiger-Muller detectors can not distinguish between radiation of different energies, but instead function as counters of radiation induced events.

Scintillation counters rely on incident radiation to excite a substance with luminescent properties, generating visible light which can then be detected by a photomultiplier tube (PMT). The system consists of a scintillation material, an optical transmisssion system to channel the light to the photomultiplier, and the PMT itself which converts the incident photons into an electrical current.

Difficulties involving the use of radiotracers in the CGF environment include determining a specific tracer, what amount, and which detection system to use for optimum performance. It is unlikely that a radiotracer could be deployed within the ampoule due to possible interference with the crystalline compound, but it could be used in the cartridge. The sensitivity of the method would depend on the amount of tracer used, its dilution in the cartridge, and the background radiation level already present. However, like the PFT technique, this approach would be unable to determine which cartridge had failed without using completely different radioisotopes in each. This would also necessitate an equal number of detection systems be located within the EAC. However, the most important issue concerning the use of radiotracers is safety. It would be illogical and impractical to introduce a tracer into the CGF environment which itself could present a safety hazard to the crew.

## 3.3 Detection Methods in the EAC

### 3.3.1 Mass Spectrometry

Mass spectrometers are widely used in pollution studies, toxicology, and leak detection due to their high sensitivity and resolution. An important analytical tool, they can determine the exact composition of a gas in a system. Simply, mass spectrometers separate and record the masses of ionized atoms.

The molecules of a gas enter into a mass spectrometer, which operates under a high vacuum and are then passed through an ionization chamber. Electron bombardment is the most prevalent form of ionization, using a tungsten filament electrically heated to around 2000 °C. The resulting electron beam collides with the incoming gas molecules and produces primarily positive ions. Subsequently, these ions are accelerated through an electric field with a potential difference of 800 to 8000 volts before entering a magnetic field analyzer.

After complete acceleration, the potential energy of the ions equals the kinetic energy. Additionally, once inside the magnetic field, the ions are subjected to centripetal and centrifugal forces in equilibrium. These two relationships result in a trajectory radius of curvature that is a function of the mass-to-electric charge ratio of an ion. Thus, when the magnetic field

curves the ion trajectories, all ions with the same mass-to-electric charge ratio fall into the same path. These beams of similar ions are then passed through a slit leading to the collector.

In a spectrometer, the ion beams incident on the collector create an electric current with an intensity proportional to the number of ions arriving. By using a very sensitive current gauge, the mass spectrometer can record a single ion. Each response will result in its own peak, the record of these signals constituting the mass spectrum. Normally arranged in order of the lowest mass to the highest, each peak mass number corresponds to a molecular weight. High resolution mass spectrometers can establish the exact molecular weight and, therefore, the empirical formula of the gaseous constituents. This is usually accomplished by the use of a reference ion, or a library file when the mass spectrum is sent to a computer.

Operating in much the same way as the magnetic mass spectrometer described above is the quadrupole. However, instead of using a magnetic field to separate the ions, the quadrupole mass spectrometer uses applied DC and radiofrequency (RF) potentials of opposite signs to create two fields within the analyzer. Entering ions are separated according to both the mass-to-charge and the RF/DC ratios. For each value of these ratios, only one mass is able to pass through the analyzer to the

collector. Therefore, a single constituent may be may be selected, or the ratios may be varied to scan the entire spectrum.

The mass spectrometer's main advantage is that it is a proven technology that is used extensively. Both highly sensitive and dependable, it can also be adjusted to detect specific molecular compounds of interest. Yet applying this technology to the constraints of the EAC environment would present a number of difficulties. Since the mass spectrometer must operate under a high vacuum, the required internal equipment makes the instrument too large to fit inside the EAC. The device would need to be located outside the experiment and also connected to a computer for analysis of collected data. An additional disadvantage is that molecules must be in the gaseous phase to be detected. Some of the hazardous crystal constituents do not exist in significant vapor phase concentrations at ambient temperatures such as those in the EAC. Also, to avoid plumbing the EAC for the mass spectrometer connection, it would be necessary to extract gas samples from the vent line that leads overboard. However, this would bring possible contaminants into the shuttle/station substructure. In addition, the critical constituents would have even more area to deposit on before diffusing to the detector.

### 3.3.2 Spark Source Emission Spectroscopy

As mentioned previously, metallic elements may be detected in sub-parts per million levels through SSES. Detection is achieved using a polychromator to look for specific emission lines in a spark-induced plasma, coupled with a solid state array detector such as a CID for a wide spectral coverage and high sensitivity. Although the bulky instrumentation and high-voltage spark associated with this method render it unsuitable for use within the cartridge, it does show promise for contamination monitoring within the EAC.

Among the several advantages offered by SSES are its low limits of detection, commercial availability, and species-specific nature. Given that each ampoule contains a slightly different composition, it would be possible to determine precisely which SACA has failed. An added benefit is that detection of metallics is not limited to the crystal growth species. Outgassed material from thermocouples and other hardware inside the EAC could also be quantified, thereby detecting any erosion of the CGF components. Also, unlike MS, SSES implementation does not necessitate plumbing the EAC.

The most probable configuration for EAC monitoring would be to station a small spark source inside the EAC in front of the viewport, and locate the detection equipment outside the EAC, looking through the opposite side of the

viewport. This arrangement would require that only the spark source be directly connected to the experiment, and then it would be sealed within the EAC environment with no leads to the outside. The emitted radiation would travel through the window to a collection lens and fiber optic or other such transmission system.

The proposed polychromator is a Paschen-Runge design using a concave diffraction grating. The grating separates the incoming light into two physical dimensions according to wavelength. The detector, a liquid nitrogen or thermoelectrically cooled CID, then captures the two dimensional spectral map. A thermoelectric cooling approach would be the most practical for CGF conditions. Output from the array is digitized and may be analyzed on the ground or on board computers.

The two primary disadvantages of this approach are the high-voltage spark and sizable instrumentation requirements. However, these aspects of the method may be modified in ways that would minimize their impact, as discussed below.

The high-voltage spark produces radio frequency and electromagnetic emissions while generating the high-temperature plasma, emissions which could interfere with the growth process of the crystalline compounds under study. If this proves to be a problem, there are at least two possible solutions. First, the spark generator could

be shielded on all sides except the side facing the detector. Secondly, a schedule could be adopted where testing of the EAC environment would not overlap with sample processing.

The unwieldy instrumentation commonly associated with SSES contains many peripheral components non-essential to EAC monitoring. Commercially available SSES systems include a dedicated computer and cabinet space, items which may be eliminated. The polychromator is the only critical element requiring considerable space. Current advanced designs allow minimizing dimensions of a high performance polychromator to not more than 500 by 300 by 200 mm. Although this is probably still too sizable to be placed within the EAC, a radiation transmission system would enable a polychromator to operate effectively outside the EAC. For instance, using fiber optics to transmit the light would allow the polychromator to be placed a considerable distance from the CGF assembly.

## 3.4 Summary of Detection Methods

The following tables attempt to summarize the leak detection methods detailed in the previous sections by separating them into two categories: those that may be able to conform to the special constraints of this

experiment and provide adequate leak detection, given in Table 3.4(a); and those that are for some reason or reasons unsuited for use within the CGF system, listed in Table 3.4(b).

| Method of Detection | Level of Detection | Limit of Detection | Response Time |
|---|---|---|---|
| Surface Reflectance | ampoule | (qualitative) | undetermined |
| Make-Wire Sensor | ampoule | (qualitative) | undetermined |
| Pressure Measurement: | cartridge/ ampoule | | |
| Piezo-transducer | | 0.25 kPa | < 1 ms |
| Fiber Optic | | 0.70 kPa | < 1 ms |
| SSES | SACA (in EAC) | < ppm | undetermined |

Table 3.4(a): Potential Leak Detection Methods

| Method of Detection | Reason Unfeasible |
|---|---|
| Ampoule Failure Detection: | |
| AAS | excessive instrumentation requirements, insufficient resolution |
| Electro-chemical Sensor | insufficiently developed technology |
| Ultrasonics | possible interference with crystal growth, failure above 575°C |
| Microbalance | sensitive to outgassed materials, failure above 450°C |
| Cartridge Failure Detection: | |
| Tracer: | need multiple tracers to distinguish which cartridge has failed, and subsequently more detection equipment |
| PFT | cannot exist above 500°C |
| Radiotracer | possible safety hazard |
| SACA Failure Detection in EAC: | |
| MS | too large to fit inside EAC, and cannot plumb EAC |

Table 3.4(b): Unsuitable Leak Detection Methods

Note that in Table 3.4(a), response times are given for the detection instrument only. Actual response times for the pressure measurement techniques would be dependent on how long it took for the internal cartridge pressure to change by the specified limit of detection. This is addressed in section 4.2 of this report. Limits of detection for the pressure measuring devices are also dependent on the range of the particular gauge chosen. Response times for other methods, listed as undetermined, would be highly dependent on sample vapor transport and deposition processes. The effectiveness of cartridge-based methods that rely on direct sensing of the sample is discussed in section 5.1.

# 4.0 ANALYSES

## 4.1 Thermodynamic Analysis

### 4.1.1 Sample Deposition

An ampoule failure will result in two occurrences: the deposition of sample material onto the cartridge walls and packing, and an increase in the total cartridge pressure. A simple thermodynamic analysis was conducted to determine where such an escaped species would deposit, and the pressure increase that could be expected in the cartridge.

Regarding deposition, metallic species that escape from a broken ampoule will deposit onto surfaces that are at a temperature lower than the dew point temperature of the vapor. The dew point temperature was calculated using a Clausius-Clapeyron relation:

$$\log(P) = -0.05223 \times \frac{a}{T} + b$$

(*Handbook of Chemistry and Physics*, 1992-1993)

where P is the vapor pressure of the species, T is the dew point temperature, and a and b are constants specific to

the volatile species within the sample. Values of a and b for the volatile species studied, as well as the vapor pressures for those constituents, are provided in Appendix C.

### 4.1.2 Effect of Ampoule Failure on Pressure

The increase in cartridge pressure resulting from an ampoule failure was calculated by summing the increase in mass within the cartridge due to the escaped species.

$$[\text{Mass}]_{\text{total}} = [\text{Mass}]_{\text{argon}} + [\text{Mass}]_{\text{species}}$$

The argon already present within the cartridge was assumed to be displaced by the sample. The following formula, derived from ideal gas law, was used to estimate the change in cartridge pressure:

$$\Delta P = \frac{T_c}{V_c} \times \int \frac{P(x)}{T(x)} A(x)\, dx$$

where $T_c$ is the weighted average temperature of the cartridge, $V_c$ is the total cartridge volume, $P(x)$ and $T(x)$ are the locational vapor pressure and temperature of the sample, and $A(x)$ is the open cross sectional area of the cartridge at that location. The open cross sectional area for each cartridge was estimated using a NASA engineering drawing of that SACA, an example of which is provided in

Figure 4.1. P(x) was assumed to be the vapor pressure of the volatile component above the compound until the temperature fell below the dew point temperature, when P(x) was calculated using the Clausius-Clapeyron equation specified above. The volatile component may be identified as the component having the highest vapor pressure relative to the compound and the other component or components comprising of the compound. The vapor pressure of the volatile constituent above the compound is governed by the equilibrium vapor pressure of that constituent at the temperature at that location. Additionally, $T_c$ may be defined with the following formula:

$$T_c = \left(\frac{1}{L_c} x \sum_{i=1}^{N} \frac{L_i}{T_i}\right)^{-1}$$

where $L_c$ is the length of the cartridge, $L_i$ is the length of segment i, and $T_i$ is the average temperature of segment i. N represents the number of segments, which are as follows: hot zone, adiabatic zone, cold zone, and the segment from the cold zone to the cartridge cap.

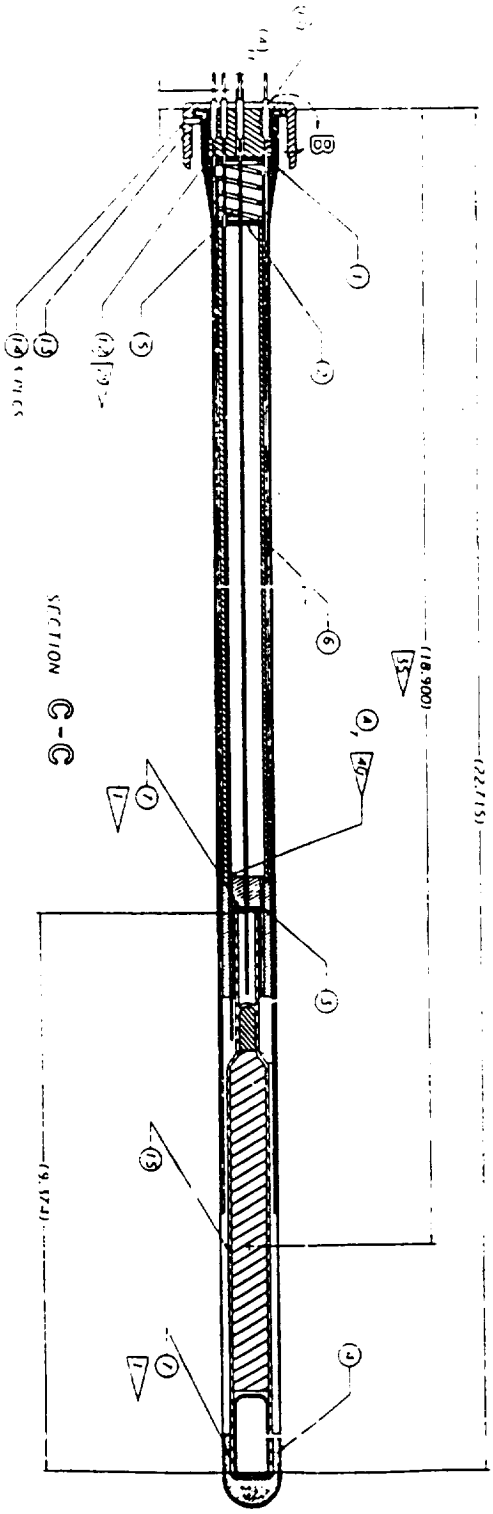

Figure 4.1: CdZnTe SACA Engineering Drawing

(NASA/MSFC Drawing Number 96M65357)

## 4.2 Pressure Sensitivity Analysis

A pressure sensitivity analysis was conducted to estimate the response times of a detection method based on pressure measurement in the event of a cartridge failure. A hole in the wall of the cartridge was modelled as a converging nozzle on the inside of the cartridge, in series with a duct through the wall opening to the EAC environment. Flow through the nozzle was assumed to be isentropic, and Fanno flow relations were used through the duct.

A computer program was used to solve the relations, using an iterative approach until specified conditions at the duct exit were satisfied. By comparing the Fanno length L*, the length necessary for choked flow through the duct, to the actual duct length, one of two exit conditions was used. If L* was less than or equal to the duct length, the mach number at the exit was set equal to one. For the case where L* was greater than the duct length, the iteration was continued until either the exit pressure equaled the back pressure, or the value of L* decreased to the duct length. A Colebrook friction factor was used, based on the Reynolds number at the duct entrance and the pipe roughness, and evaluated using Newton's method of iteration. A listing of the program is given in Appendix E of this report.

The time required for the cartridge pressure to change by a specified percent was then calculated by combining the definitions of mass flow rate and the ideal gas law to yield:

$$\Delta t = \frac{V}{mRT_o} \times \Delta P_o$$

where t is the time in seconds, V is the flow velocity at the duct entrance, $\Delta P_o$ and $T_o$ are the change in cartridge pressure and temperature within the cartridge respectively, m is the mass flow rate through the duct, and R is the gas constant.

## 5.0 Results and Discussion

### 5.1 Sample Deposition

Figures 5.1(a) through 5.1(d) illustrate temperature profiles during processing for each of the United States Microgravity Laboratory -1 (USML-1) experiments, as well as the dew point temperature for the relevant sample species and its relative position within the cartridge. The figures indicate a point of deposition of an escaped species, measured from the cartridge cap, ranging from 2.32cm for GaAs to 43.6cm for HgZnTe. As illustrated by the graphs, these results are highly dependent on the temperature profile within the cartridge and the specific sample being processed. Thus, if an experiment were at a different point in its processing stage, the temperature profile, and subsequently, the point of deposition, would change. Additionally, since the dew point temperature is specific to a given species, any two experiments with the same temperature profile but different samples would also have different deposition locations.

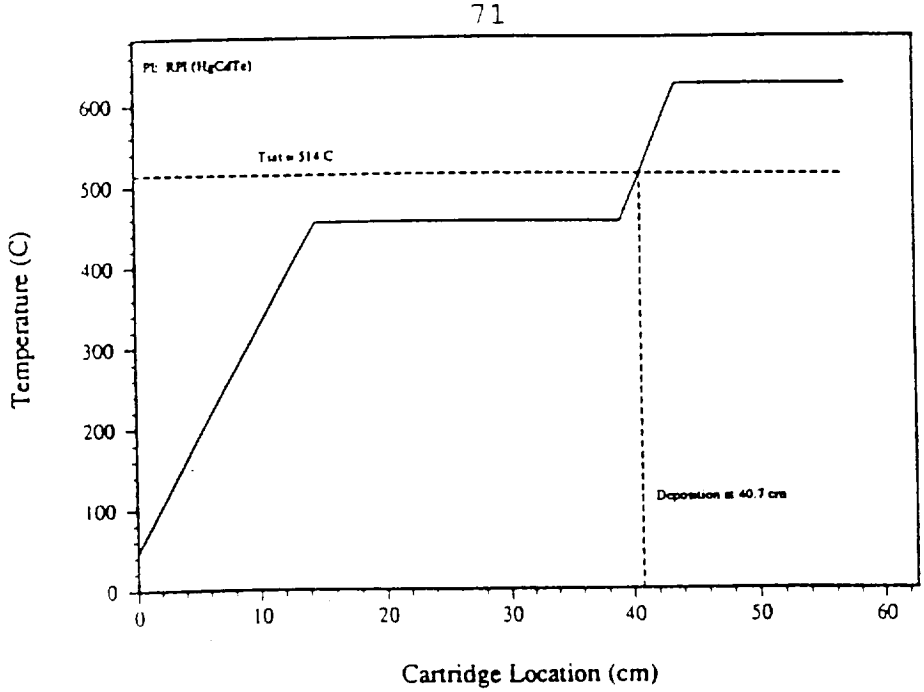


Figure 5.1(a): HgCdTe SACA Temperature Profile and Dew Point Location

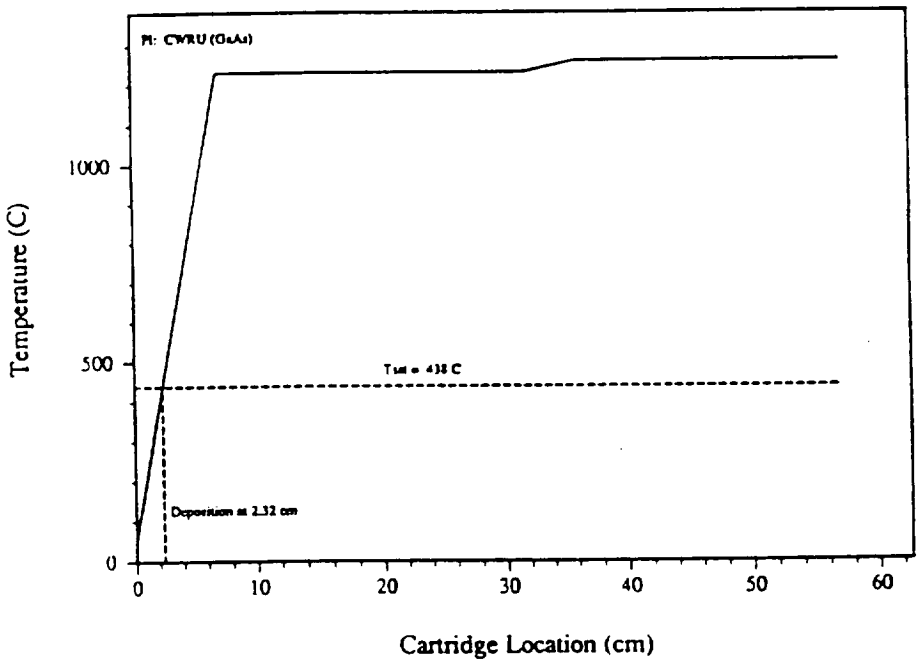


Figure 5.1(b): GaAs SACA Temperature Profile and Dew Point Location

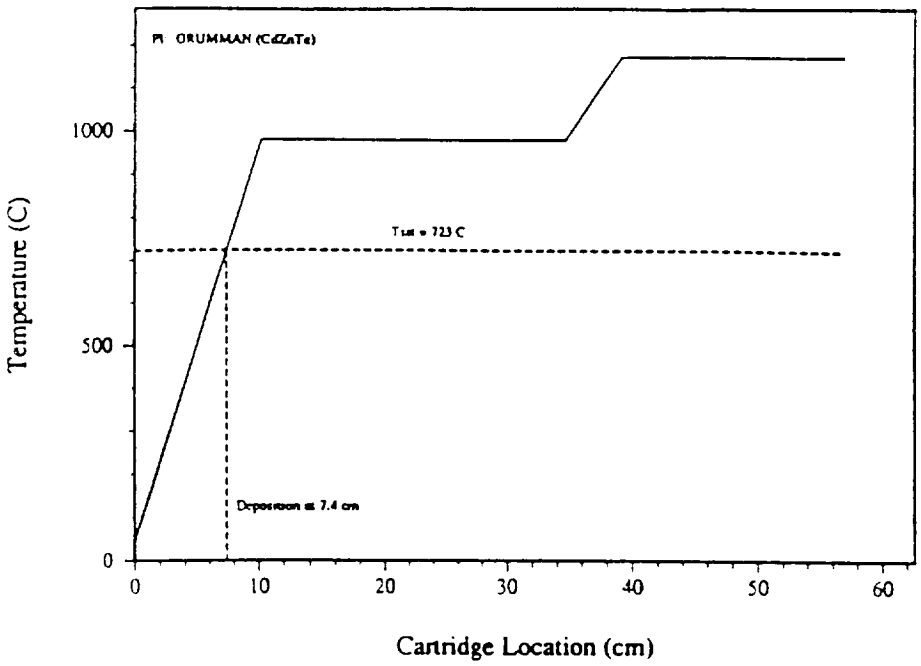


Figure 5.1(c): CdZnTe SACA Temperature Profile and Dew Point Location

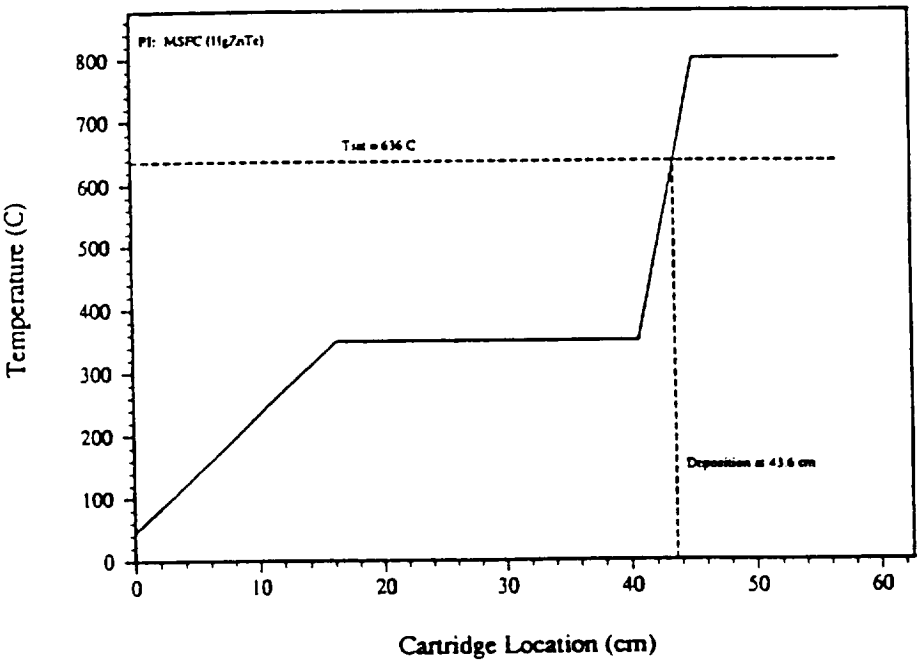


Figure 5.1(d): HgZnTe SACA Temperature Profile and Dew Point Location

## 5.2 Effect of Ampoule Failure on Pressure

The changes in cartridge pressure due to an ampoule failure were calculated using the methodology specified in section 4.2. Results for the increase in internal cartridge pressure at processing conditions for each sample flown on USML-1 are summarized in Table 5.2.

| | HgCdTe | GaAs | CdZnTe | HgZnTe |
|---|---|---|---|---|
| $P_{cart,proc}$ (kPa) | 101.33 | 227.53 | 101.33 | 101.33 |
| $\Delta P$ (kPa) | 218.7 | 171.0 | 42.1 | 457.7 |
| % Increase | 216 % | 75 % | 42 % | 452 % |

Table 5.2: Cartridge Pressure Increase Due to Ampoule Failure for USML-1 Experiments

## 5.3 Pressure Sensitivity

Cases were run for each of the experiments flown on USML-1, using processing conditions. Graphs illustrating response times as a function of hole diameter for each of the USML-1 experiments are shown in Figures 5.3(a) through 5.3(d). Table 5.3(a) highlights some response times for selected hole diameters for a $\Delta P/P$ of 2.0%.

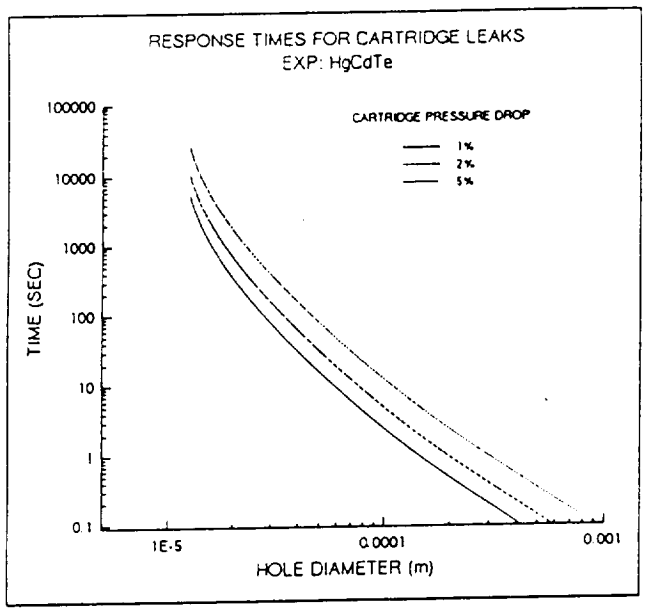


Figure 5.3(a): Response Time as a Function of Hole Diameter for the HgCdTe SACA

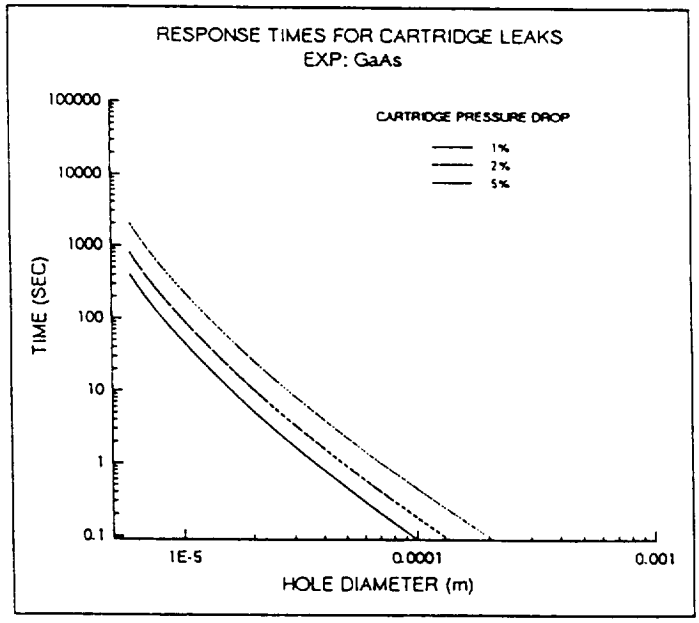


Figure 5.3(b): Response Time as a Function of Hole Diameter for the GaAs SACA

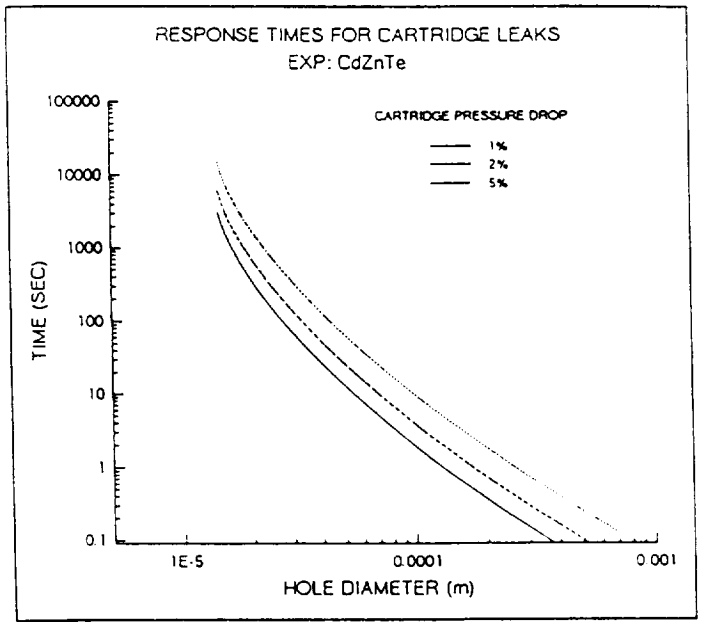


Figure 5.3(c): Response Time as a Function of Hole Diameter for the CdZnTe SACA

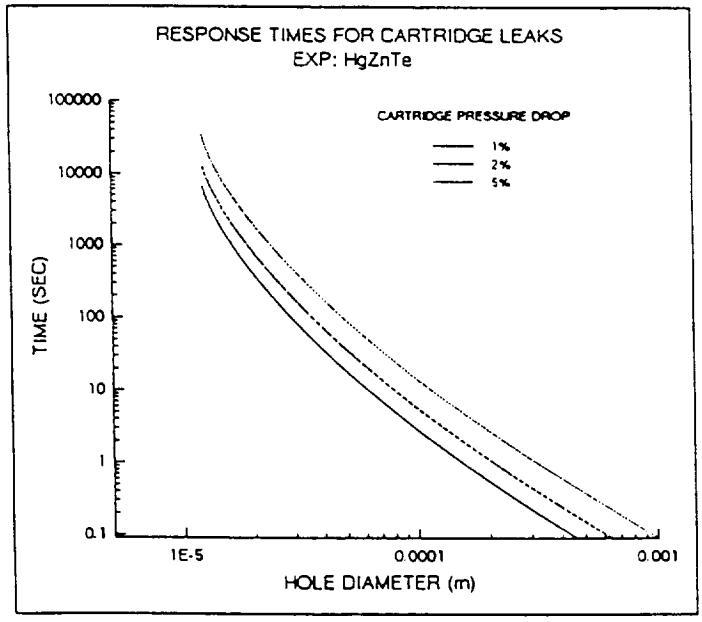


Figure 5.3(d): Response Time as a Function of Hole Diameter for the HgZnTe SACA

| | Response Time (sec) | | | |
|---|---|---|---|---|
| Diameter(m) | HgCdTe | GaAs | CdZnTe | HgZnTe |
| 1.4E-5 | 3638.0 | 29.0 | 6312.0 | 3864.0 |
| 1.0E-4 | 4.7 | 0.2 | 3.8 | 5.6 |
| 1.0E-3 | 0.03 | >0.01 | 0.02 | 0.04 |

Table 5.3(a): Response Times for Selected Hole Diameters on USML-1 Experiments

For three out of the four experiments flown on USML-1, the internal cartridge pressure during processing reached 101.325 kPa. Specifically, these experiments were HgCdTe, CdZnTe, and HgZnTe. During this time interval, the EAC pressure was maintained at 96.0 kPa. Increasing the pressure differential across the cartridge and EAC would obviously decrease the time required for a specified change in cartridge pressure. Cases were therefore run on one of the cartridges using different internal pressures and then calculating the response times. Figures 5.2(e) through 5.2(g) demonstrate the effect of decreasing the internal cartridge pressure while holding all other factors constant for a HgZnTe sample flown on USML-1. Results demonstrated a 82% decrease in detection time when decreasing the original internal cartridge pressure at

processing conditions by only 18.6 kPa. A brief summary of the response times for selected hole diameters at a $\Delta P/P$ of 2.0% is given in Table 5.3(b).

| | Response Time (sec) | | | |
|---|---|---|---|---|
| Diameter(m) | 101.33kPa | 82.74kPa | 68.95kPa | 55.16kPa |
| 1.2E-5 | 13542.0 | 2434.0 | 966.0 | 561.0 |
| 1.0E-4 | 5.6 | 3.1 | 1.9 | 1.3 |
| 1.0E-3 | 0.04 | 0.02 | 0.01 | 0.01 |

Table 5.3(b): Response Times for the HgZnTe Experiment for Different Internal Cartridge Pressures

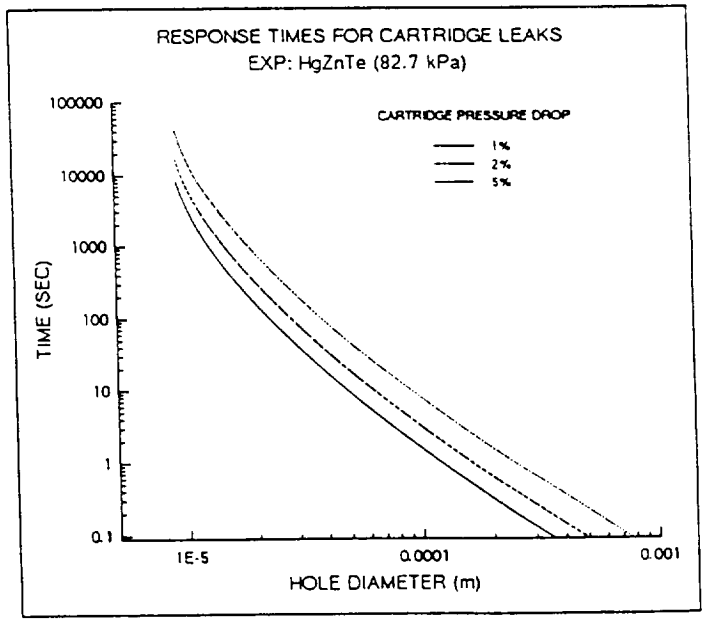


Figure 5.3(e): Response Times for HgZnTe Experiment with 82.737kPa (12psi) Cartridge Pressure

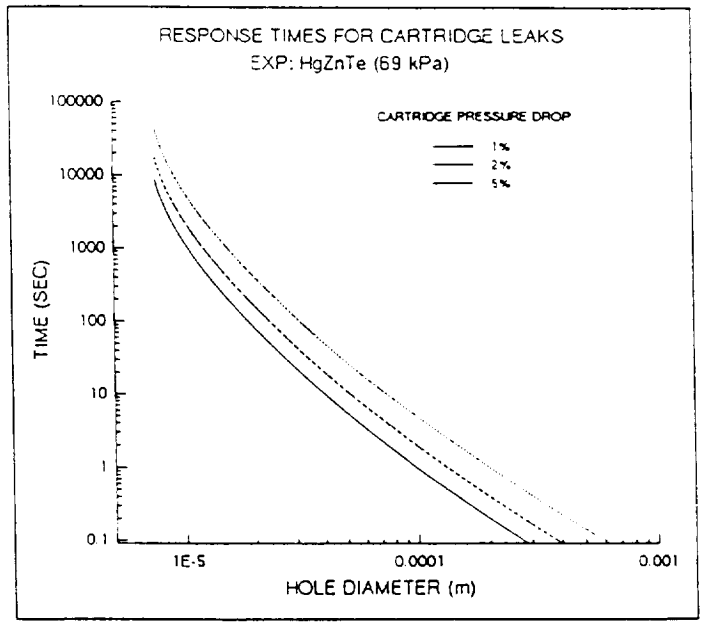


Figure 5.3(f): Response Times for HgZnTe Experiment with 68.949kPa (10psi) Cartridge Pressure

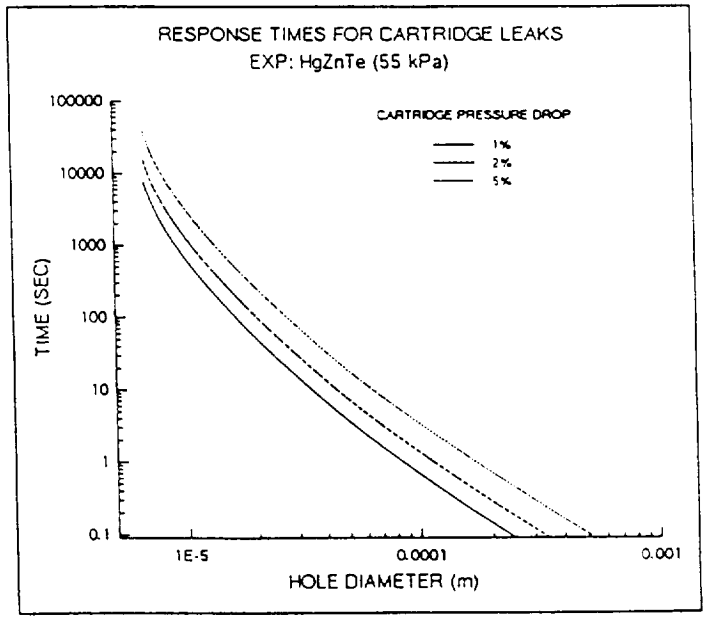


Figure 5.3(g): Response TImes for HgZnTe Experiment with 55.158kPa (8psi) Cartridge Pressure

## 6.0 CONCLUSION

The results of the thermodynamic analysis highlight two issues of vital importance to safety considerations regarding the SACA . First, the success of any leak detection method based on sample deposition is dependent on its location within the cartridge. For instance, the make-wire sensor would need to be located at a position where the temperature in the cartridge reaches the dew point temperature of the volatile species. If the sensor is at a temperature higher than the dew point, the sample vapor will not deposit, and therefore not be detected. Conversely, if the sensor is located at a temperature below the dew point, but at a position far enough removed from where that temperature is first reached, the species could deposit out onto the cartridge walls and packing, and thus never reach the sensor. An additional complication to this positional sensor dependence is that the location of the dew point temperature within the cartridge varies with time as the furnace is translated during processing. Any deposition sensor would therefore need to be positionally independent. For example, a

sensor would need to be fabricated in the form of a continuous strip running the length of the cartridge instead of a miniaturized, discrete unit.

Another safety concern resulting from the thermodynamic analysis is the magnitude of the pressure increase within the cartridge in the event of an ampoule failure. For one sample, an ampoule failure resulted in a 400% increase in cartridge pressure at processing conditions. Cartridge integrity under these circumstances needs to be assured. One advantage to such a pressure increase, however, is that it would be easily detectable by a pressure measurement technique.

Additionally, the pressure sensitivity analysis demonstrates that response times for detecting a cartridge failure can be significantly reduced by increasing the pressure differential across the cartridge to the EAC. Creating such a negative cartridge pressure differential with respect to the EAC would be desirable in terms of a cartridge level of containment. However, in the event of an ampoule failure, the cartridge pressure would be much greater than that of the EAC. This means that a species escaped from an ampoule would still be driven out of the cartridge should the cartridge also fail, despite a reduced cartridge internal pressure. Therefore, reducing the cartridge internal pressure would serve to reduce the

response time for detecting cartridge failure, but would not likely be of any benefit were the ampoule to also fail.

In summary, any ampoule failure detection method based on sample deposition needs to be able to withstand the maximum processing temperature of a sample, since it will need to detect a crystal growth species at any point along the length of the cartridge. Any such method must also demonstrate an ability to withstand outgassing by other SACA materials, such as thermocouples, without yielding false positive detection results. Additionally, while a pressure measurement detection method would appear to effectively warn of a cartridge or ampoule failure, one issue needs to be addressed. Since the pressure within the cartridge naturally increases with increasing temperatures during processing, the monitoring system would need to be supplemented with a supporting computer code which would define the normal parameters of this increase, and warn of a failure only when the cartridge pressure fell or rose outside this range. These parameters could be estimated given the known furnace ramp-up and ramp-down times and the furnace translation rate, but the accuracy of such a code would be dependent on the reliability of the heating rate within the furnace.

## 7.0 REFERENCES


Alcock, C.B.; Li, Baozhen; Fergus, J.W.; and Wang, Li. "New Electrochemical Sensors for Oxygen Determination", *Solid State Ionics*, 1992, 39-43.

Arnold, Niel S.; McClennen, William H.; and Meuzelaar, Henk L.C. "Vapor Sampling Device for Direct Short Column Gas Chromatography/Mass Spectrometry Analyses of Atmospheric Vapors", *Analytical Chemistry*, Vol. 63, No. 3, February 1991, 299-304.

Beauchemin, Diane; Le Blanc, J.C. Yves; Peters, Gregory R.; and Craig, Jane M. "Plasma Emission Spectroscopy", *Analytical Chemistry*, Vol. 64, No. 12, June 1992, 442R-467R.

Blyler, L.L.; Lieberman, R.A.; Cohen, L.G.; Ferrara, J.A.; and MacChesney, J.B. "Optical Fiber Chemical Sensors Utilizing Dye-Doped Silicone Polymer Claddings", *Polymer Engineering and Science*, Vol. 29, No. 17, September 1989, 1215-1218.

Butler, M.A.; Ricco, A.J.; and Buss, R. "Fiber Optic Micromirror Sensor for Volatile Organic Compounds", *J. Electrochemical Society*, Vol. 137, No. 4, April 1990, 1325-1326.

Carson, B.L., Ellis III, H.V., and McCann, J.L.: *Toxicology and Biological Monitoring of Metals in Humans*,Lewis Publishers Inc.,Chelsea, Michigan, 1986.

Dietz, R.N. "Commercial Applications of Perfluorocarbon Tracer Technology", June 1991: presented at the Department of Commerce Environmental Conference, "Protecting the Environment: New Technologies – New Markets", Reston, VA, 5-6 September 1991.

Dietz, R.N. "Perfluorocarbon Tracer Technology", in: *Regional and Long-range Transport of Air Pollution*, Lectures of a course held at the Joint Research Centre, Ispra, Italy, 15-19 September 1986, S. Sandroni (Editor), 215-247, Elsevier Science Publishers B.V., Amsterdam, The Netherlands, 1987.

Dietz, Russell N.; and Goodrich, Robert W. "Demonstration of Rapid and Sensitive Module Leak Certification for Space Station Freedom: Final Report", prepared for NASA/MSFC, March 1991.

Dietz, Russell N.; and Senum, Gunnar I. "Capabilities Needs, and Applications of Gaseous Tracers", in: Atmospheric Tracer Workshop, Santa Fe, NM, May 21-25, 1984, Los Alamos National Laboratories, LA-10301-C, December 1984, 123-173.

D'Ottavio, Ted W.; Goodrich, Robert W.; and Dietz, Russell N. "Perfluorocarbon Measurement Using an Automated Dual-Trap Analyzer", *Environmental Science snd Technology*, Vol. 20, No. 1, 1986, 100-104.

Fields, Robert E.; and Denton, M. Bonner. "Array Detectors Expand Atomic Spectroscopy", *Laser Focus World*, March 1992, 107-113.

Foldiak, G. (Editor): *Industrial Applications of Radioisotopes*, Elsevier Science Publiching Co., New York, 1986.

Frigerio, Alberto: *Essential Aspects of Mass Spectrometry*, Spectrum Publications Inc., New York, 1974.

Gabrielli, C.; Keddam, M.; and Torresi, R. "Calibration of the Electrochemical Quartz Crystal Microbalance", *J. Electrochem. Soc: Electrochemical Science and Technology*, Vol. 138, No. 9, September 1991, 2657-2660.

Hall, James E. "Silicon Sensors Upgrade Pressure Measurements", *InTech*, July 1991, 32-33.

*Handbook of Chemistry and Physics*, 73rd edition. Boca Raton, Florida: Chemical Rubber Publishing Co., 1992-1993.

Harte, John, Holdren, C., Schneider, R., and Shirley, C.: *Toxics A to Z: a guide to everday pollution hazards*, University of California Press, Los Angeles, 1991.

Henderson, P.J.; Spencer, J.; and Jones, G.R. "Pressure Sensing Using a Chromatically Addressed Diaphragm", *Measurement Science Technology*, Vol. 4, 1993, 88-94.

Hershey, J.Wilson; and Keliher, Peter N. "Observations on Arsenic and Selenium Determinations Using Hydride Generation Atomic Absorption and/or Plasma Emission Spectroscopy", *Applied Spectroscopy Reviews*, 1989-90, 213-228.

Hughes, R.C.; Ricco, A.J.; Butler, M.A.; and Martin, S.J. "Chemical Microsensors", *Science*, Vol. 254, October 1991, 74-80.

Johnson, M.L., and Galloway, P.N.: Metal vapor or electronic semiconductor material sensor/detector. NASA disclosure of Invention, NASA/MSFC, 1990.

Ketar, S.N.; Penn, S.M.; and Fite, W.L. "Real-Time Detection of Parts per Trillion Levels of Chemical Warfare Agents in Ambient Air Using Atmospheric Pressure Ionization Tandem Quadrupole Mass Spectrometry", *Analytical Chemistry*, Vol. 63, No. 5, March 1991, 457-459.

Kistler Corporation: Piezo-Insrumentation general catalogue K2.006, First Edition, September 1989.

Kistler Corporation: Piezoresistive Measuring Instruments catalogue, 1993.

Kleinknecht, Konrad: *Detectors for Particle Radiation*, Cambridge University Press, Cambridge, 1986.

Majidi, Vahid; Rae, Jay T.; and Ratliff, Judy. "Determination of Trace Metals Using an Electrothermal Atomizer by Laser-Induced Plasma Atomic Emission Spectrometry", *Analytical Chemistry*, Vol. 63, No. 15, 1600-1602.

Moslehi, Behzad; Shahriari, Mahmoud R.; Schmidlin, Edward M.; Anderson, Mojdeh; and Lukasiewicz, Michael A. "Optical Fiber Simplifies Gas-Sensing Systems", *Laser Focus World*, April 1992, 161-168.

Murphy, M.M.; and Jones, G.R. "Optical Fibre Pressure Measurement", *Measurement Science Technology*, Vol. 4, 1993, 258-262.

Narayanaswamy, R.; and Sevilla, F. III. "Optical Fibre Sensors for Chemical Species", *J. of Physics E.*, Vol. 21, 1988, 10-17.

NASA/MSFC: ICD-2-60026, "CGF Experiment Cartridge Interface to the P.I. Sample/Ampoule Assembly – Crystal Growth of Selected II - IV Semiconducting Alloys by Directional Solidification", March 1990

NASA/MSFC: ICD-2-60027, "CGF Experiment Cartridge Interface to the P.I. Sample/Ampoule Assembly – The Study of Dopant Segregation Behavior During Growth of GaAs in Microgravity", March 1990.

NASA/MSFC: ICD-2-60028, "CGF Experiment Cartridge Interface to the P.I. Sample/Ampoule Assembly – Vapor Transport Crystal Growth of HgCdTe in Microgravity", March 1990.

NASA/MSFC: ICD-2-60029, "CGF Experiment Cartridge Interface to the P.I. Sample/Ampoule Assembly – Orbital Processing of High Quality CdTe Compound Semiconductors", March 1990.

NASA/JSC: NSTS 1700.7B, "Safety Policy and Requirements for Payloads Using the Space Transportation System", January 1989.

Photonetics, Inc.: Fiber optic pressure sensor product description, 1993.

Radziemski, Leon J.; Loree, Thomas R.; Cremers David A.; and Hoffman, Nelson M. "Time-Resolved Laser Induced Breakdown Spectrometry of Aerosols", *Analytical Chemistry*, Vol. 55, No. 8, July 1983, 1246-1252.

Rosentreter, Jeffrey J.; and Skogerboe, Rodney K. "Trace Determination and Speciation of Cyanide Ion by Atomic Absorption Spectroscopy", *Analytical Chemistry*, Vol. 63, N0. 7, April 1991, 682-688.

Sarrafzadeh, A.; Churchill, R.J.; and Niimura, M.G. "Laser Generated Ultrasound", *Acousto-Ultrasonics: Theory and Application*, edited by John C. Duke, Jr., Plenum Press, New York, 1988.

Shapiro, Ascher H.: *The Dynamics and Thermodynamics of Compressible Fluid Flow*, John Wiley & Sons, New York, 1953.

Sinha, Mahadeva P.; and Gutnikov, George. "Development of a Miniaturized Gas Chromatograph-Mass Spectrometer with a Microbore Capillary Column and an Arayy Detector", *Analytical Chemistry*, Vol. 63, No. 18, September 1991, 2012-2016.

Sotera, J.J.; and Khan, H.L. "Background Correction in AAS", *American Laboratory*, November 1982.

Szilard, J. (Editor): *Ultrasonic Testing: Non-Conventional Testing Techniques*, John Wiley & Sons, New York, 1982.

Teledyne Brown Engineering: Memorandum MEPF-CGF 2/93-311, "Ampoule Positions and Temperatures for USML-1", Shelley Le Roy to Srini Srinivas, October 15, 1993.

Teledyne Brown Engineering: SP-DOC-6102, "Design and Development of the Multiple Experiment Processing Furnace: System Design Description", Contract Number NAS8-36637, March 1990.

Teledyne Brown Engineering: SP-RPT-6752, "Design and Development of the Multiple Experiment Processing Furnace: Reconfigurable Furnace Module Thermal Analysis Report", Contract Number NAS8-36637, April 1991.

Thermo Jarrell Ash Corporation; AVA 880 product description, 1992.

Van Veen, Eric H.; and de Loos-Vollebregt, Margaretha T.C. "Determination of Trace Elements in Uranium by Inductively Coupled Plasma-Atomic Emission Spectrometry Using Kalman Filtering", *Analytical Chemistry*, Vol. 64, No. 15, August 1992, 1643-1649.

Ward, Michael, D.; and Buttry, Daniel A. "In Situ Mass Detection with Piezoelectric Transducers", *Science*, Vol. 249, 1990, 1000-1007.

Wiemhöfer, Hans-Dieter; and Göpel, Wolfgang. "Fundamentals of Potentometric Gas Sensors Based upon Solid Electrolytes", *Sensors and Actuators*, 1991, 365-372.

Wilcox, William R. (Editor): *Preparation and Properties of Solid State Materials*, Volume 2, Marcel Dekker Inc., New York, 1976.

Zakipour, S.; and Leygraf, C. "Studies on Electrical Contact Materials by Means of Quartz Crstal Microbalance and XPS", *J. Electrochem. Soc.: Electrochemical Science and Technology*, Vol. 133, No. 5, May 1986, 873-876.

# APPENDICES

# APPENDIX A

# ACRONYM LIST

## ACRONYM LIST

| | |
|---|---|
| AAS | Atomic Absorption Spectrometry |
| AC | Applied Current |
| AES | Atomic Emission Spectrometry |
| BATS | Brookhaven Atmospheric Tracer Sampler |
| BNL | Brookhaven National Laboratories |
| CGF | Crystal Growth Furnace |
| CID | Charge-Injection Device |
| CWRU | Case Western Reserve University |
| DC | Direct Current |
| DTA | Dual-Trap Analyzer |
| EAC | Experiment Apparatus Container |
| ECD | Electron Capture Device |
| EMF | Electromotive Force |
| ETA | Electrothermal Atomization |
| GC | Gas Chromatography |
| GRU | Grumann |
| ICP | Inductively Coupled Plasma |
| IFEA | Integrated Furnace Assembly |
| LED | Laser Emitting Diode |

| | |
|---|---|
| MW | Make-wire (sensor) |
| MS | Mass Spectrometry |
| MSFC | Marshall Space Flight Center |
| NASA | National Aeronautics and Space Administration |
| NOAA | National Oceanographic and Atmospheric Association |
| PI | Principle Investigator |
| PCS | Plastic-Clad, Fused-Silica |
| PFT | Perfluorocarbon Tracer |
| PMT | Photomultiplier Tube |
| QCM | Quartz-Crystal Microbalance |
| RF | Radiofrequency |
| RFM | Reconfigurable Furnace Module |
| RPI | Rensselaer Polytechnic Institute |
| SACA | Sample/Ampoule Furnace Assembly |
| SEM | Sample Exchange Mechanism |
| SSES | Spark Source Emission Spectroscopy |
| SSF | Space Station Freedom |
| USML-1 | United States Microgravity Laboratory 1 |

# APPENDIX B

## SAMPLE MATERIALS/PROCESSING CONDITIONS

| **DESIGN PARAMETERS** | **HgCdTe** | **GaAs** | **CdZnTe** | **HgZnTe** |
|---|---|---|---|---|
| HOT ZONE TEMPERATURE | 625 °C | 1260 °C | 1175 °C | 800 °C |
| COLD ZONE TEMPERATURE | 455 °C | 1230 °C | 980 °C | 350 °C |
| AMPOULE INTERNAL PRESSURE | | | | |
| Ambient | 10.14 kPa (1.47 psi) | evacuated | evacuated | evacuated |
| Processing | 958.37 kPa (139.0 psi) | 227.53 kPa (33.0 psi) | 60.81 kPa (8.82 psi) | 3206.06 kPa (465.0 psi) |
| CARTRIDGE INTERNAL PRESSURE | | | | |
| Ambient | 34.47-41.37 kPa (5.0-6.0 psi) | 95.53 kPa (14.0 psi) | 20.68-27.58 kPa (3.0-4.0psi) | 27.58-34.47 kPa (4.0- 5.0 psi) |
| Processing | 101.32 kPa (14.7 psi) | 227.53 kPa (33.0 psi) | 101.32 kPa (14.7 psi) | 101.32 kPa (14.7 psi) |
| PROCESSING TIME | | | | |
| Ramp Up | 2.5 hrs | 4.25 hrs | 9.8 hrs | 6.5 hrs |
| Time at Temperature | 8.0 hrs | 14.5 hrs | 77.9 hrs | 126.5 hrs |
| Ramp Down | 5.5 hrs | 5.25 hrs | 8.3 hrs | 7.0 hrs |
| Total Time | 16-18 hrs | 29 hrs | 96 hrs | 150 hrs |
| RAMP RATE | | | | |
| Ramp Up | 250 °C/hr | 300 °C/hr | 120 °C/hr | 120 °C/hr |
| Ramp Down | 55 °C/hr | 120 °C/hr | 130 °C/hr | 95 °C/hr |

# APPENDIX C

# VOLATILE SPECIES VAPOR PRESSURES

| EXPERIMENT | VOLATILE SPECIES | VAPOR PRESSURE |
|---|---|---|
| HgCdTe | Hg | 958.371 kPa (139psi) |
| GaAs | As | 227.527 kPa (33psi) |
| CdZnTe | Cd | 60.812 kPa (8.82psi) |
| HgZnTe | Hg | 3206.062 kPa (465psi) |

| SPECIES | CLAUSIUS-CLAPEYRON CONSTANTS | TEMP. RANGE |
|---|---|---|
| As | a=47,100 b=6.692 | 800-860 °C |
| | a=133,000 b=10.800 | 440-815 °C |
| Cd | a=99,900 b=7.897 | 500-840 °C |
| | a=109,000 b=8.564 | 150-321 °C |
| Hg | a=58,700 b=7.752 | 400-1300 °C |

* Data from *Handbook of Chemistry and Physics*, 73rd edition, 1992-1993.

# APPENDIX D

# TOXICOLOGY

(NOTE: TLV-TWA is the threshold limit Value, time-weighted average for an 8 hour work day. OSHA is the Occupational Safety and Health Adminitstration.)

ARSENIC

Exposure:

Inhalation
Oral ingestion
Dermal absorption
(Although there is no evidence of direct dermal absorption for pure arsenic, some of its compounds, such as arsenic trichloride, are readily absorbed through the skin.)

Levels of Toxicity:

These vary with the valency form of the element. Trivalent arsenic compounds, inorganics such as $As_2O_3$, are the most toxic. The most toxic form of arsenic is arsine, AsH3. Inhalation of only 250 ppm may be fatal within 30 minutes.

OSHA Limits:

(Inhalation)
0.5mg As/m3 for organic compounds
0.01mg As/m3 for inorganic compounds
0.05 ppm TLV-TWA for arsine

Effects:

Inorganic compounds are skin and lung carcinogens in humans. Acute effects are usually seen only after large overdoses, and are concentrated in the gastrointestinal system. The worst case of arsenic overdose results in a systemic collapse.

CADMIUM

Exposure:

Inhalation
Oral ingestion
(No evidence of dermal absorption)

Levels of Toxicity:

Inhalation of 40-50 $mg/m^3$ of cadmium fumes during the course of one hour can prove fatal. Non-fatal pneumonitis can result from inhalation of 0.5-2.5 $mg/m^3$ per hour.

OSHA Limits:

0.2 $mg/m^3$ for cadmium dust
0.1 $mg/m^3$ for cadmium fumes

Effects:

Cadmium oxide fumes are a severe pulmonary irritant. Acute inhalation toxicity is usually characterized by a 4-10 hour delay followed by coughing and tightness in the chest area. Effects of ingestion include persistent vomiting, abdominal pain, and diarrehea occurring only 15-30 minutes after ingestion.

MERCURY

Exposure:

Inhalation
Oral ingestion
Dermal absorption

Levels of Toxicity:

Air exposure levels of 50 µg $Hg/m^3$ correspond to blood levels of 30-35 µg/L, with toxic effects occurring when blood concentrations exceed 30 µg/L.

OSHA Limits:

0.01 $mg/m^3$ for organo(alkyl)mercury
0.05 $mg/m^3$ for mercury vapor

Effects:

High levels of mercury vapor serve as a severe lung irritant and cause erosive bronchitis. Intoxication due to excessive inhalation of mercury vapor or the inorganic salts, mercurialism, first results in psychic and emotional disturbances and may cause hand tremors. Later effects are due to cummulative exposure. Acute mercury poisoning is usually caused by the inorganic salts, with early symptoms such as vomiting, shock, and in extreme cases, death.

* All toxicology information from Carson (1986) and Harte (1991).

# APPENDIX E
# FANNO FLOW PROGRAM

(Contributed by Roy J. Hartfield, 1993)

```
C     FANNO FLOW MASS FLOW PROGRAM
C
C*********************************************
C
C     REQUIRED INPUTS
C
C     GAMMA - SPECIFIC HEAT RATIO
C     MOLE - MOLECULAR WEIGHT
C     DIA - DIAMETER OF DUCT (M)
C     P0 - TOTAL PRESSURE (kPa) (IN CARTRIDGE FOR FLOW
OUT)
C     T0 - TOTAL TEMPERATURE (C) (IN CARTRIDGE FOR FLOW
OUT)
C     LENGTH - LENGTH OF HOLE (M)
C     ROUGH - SURFACE ROUGHNESS
C     PB - BACK PRESSURE (kPa) (IN CANISTER FOR FLOW OUT)
C     VIS - VISCOSITY
C     VOL - CONTAINER VOLUME (M^3)
C
      PROGRAM FANNO
      REAL GAMMA,MOLE,DIA,P0,T0,LENGTH,M1,M2,DELTAP,
          P1,P2,RHO1, V1
      REAL ROUGH,PB,VIS,FRICTION,R,AREA,PI,LSTAR1,
          LSTAR2,LTEST,RE
      REAL VOL,TIME1,TIME2,TIME5
      OPEN(UNIT=7,FILE='FANNO.DAT')
      OPEN(UNIT=6,FILE='FANNO.OUT')
      OPEN(UNIT=8,FILE='FANNO.MAS')
      OPEN(UNIT=5,FILE='CON')
C
      READ(7,*) GAMMA,MOLE,DIA,P0,T0
      READ(7,*) LENGTH,ROUGH,PB,VIS,VOL,DELPRES
C
      PI = 3.1415926
C  **  WRITE HEADER FOR OUTPUT PLOT FILE **
      WRITE(8,160)
  160 FORMAT('VARIABLES=DIA,TIME1,TIME2,TIME5',/, 'ZONE' )
```

```
      T0 = T0 + 273.16
      R = 8314.0/MOLE
      DO 300 J = 1,1000
C **  CALCULATE DIAMETERS SO THAT POINTS WILL BE EVENLY C
      SPACED ON LOG PLOT **
      DIA = (EXP(J*0.00690776))/1000000.0 + 0.000005
      AREA = PI * (DIA**2)/4.0
      DELTAP = 2.0
C
C     START ITERATION ON PRESSURE
C
      I = 0
      P1 = P0
100   P1 = P1 - DELTAP
      I = I+1
      T1 = T0 * (P1/P0)**((GAMMA - 1)/GAMMA)
      M1 = SQRT(2/(GAMMA - 1) * ((T0/T1) - 1))
      SPEED = SQRT(GAMMA*R*T1)
      V1 = M1*SPEED
      RHO1 = (P1*1000.0)/(R*T1)
      FLUX = RHO1 * V1
      RE = (FLUX * DIA)/VIS
      CALL FRICFRAC(FRICTION,RE,ROUGH)
      COEFA = (1 - M1**2)/(GAMMA * M1**2)
      COEFB = (GAMMA + 1)/(2 * GAMMA)
      COEFC = (GAMMA + 1) * M1**2
      COEFD = 2 * (1 + ((GAMMA - 1)/2 * M1**2))
      ARG = COEFA + COEFB * LOG(COEFC/COEFD)
      LSTAR1 = DIA * ARG/FRICTION
      LSTAR2 = LSTAR1 - LENGTH
      IF(LSTAR2.GT.0)GOTO 450
      IF(DELTAP.LT.0.0001)GOTO 400
      P1 = P1 + DELTAP
      DELTAP = DELTAP * 0.1
      GOTO 100
 450  CALL FANSOLV(DIA,M1,M2,GAMMA,LSTAR2,FRICTION,LTEST)
      T2 = T0 / (1 + ((GAMMA -1)/2) * M2**2)
      P2 = (FLUX/M2 * (R*T2/GAMMA)**0.5)/1000.0
      IF(P2.GT.PB)GOTO 100
      IF(DELTAP.LT.0.0001)GOTO 110
      P1 = P1 + DELTAP
      DELTAP = DELTAP * 0.1
```

```
      GOTO 100
 400  M2 = 1.0
      T2 = T0 / (1 + ((GAMMA -1)/2) * M2**2)
      P2 = (FLUX/M2 * (R*T2/GAMMA)**0.5)/1000.0

C
C ** CALCULATE RESPONSE TIMES **
C
110   TIME1 = (VOL*0.01*P0*1000.0)/(FLUX*AREA*R*T0)
      TIME2 = (VOL*0.02*P0*1000.0)/(FLUX*AREA*R*T0)
      TIME5 = (VOL*0.05*P0*1000.0)/(FLUX*AREA*R*T0)
      WRITE(8,150)DIA,TIME1,TIME2,TIME5
 300  CONTINUE
C
C  ** OUTPUT PRIMARY VARIABLES FOR FINAL DIAMETER **
      WRITE(6,130)P2
      WRITE(6,131)M2
      WRITE(6,132)FLUX*AREA
      WRITE(6,134)LSTAR1
      WRITE(6,135)LSTAR2
      WRITE(6,139)VOL
      WRITE(6,136)P1
      WRITE(6,137)T1
      WRITE(6,143)RHO1
      WRITE(6,138)FRICTION
      WRITE(6,140)M1
      WRITE(6,141)PB
      WRITE(6,142)TIME1
141   FORMAT('  PB = ', F10.5)
142   FORMAT('  TIME1 = ',F16.8)
143   FORMAT('  RHO1 = ',F16.5)
130   FORMAT('  P2 = ', F10.5)
131   FORMAT('  M2 = ', F10.3)
132   FORMAT('  MASS FLOW = ', F12.5)
134   FORMAT('  LSTAR1 = ',F10.6)
135   FORMAT('  LSTAR2 = ',F10.3)
136   FORMAT('  P1 = ',F10.3)
137   FORMAT('  T1 = ',F10.3)
138   FORMAT('  FRICTION = ',F10.6)
139   FORMAT('  VOL = ',F10.5)
140   FORMAT('  M1 = ', F10.2)
```

```
150   FORMAT(F12.9,1X,F12.4,1X,F12.4,1X,F12.4)
      STOP
      END




      SUBROUTINE FANSOLV(DIA,M1,M2,GAMMA,LSTAR2,
          FRICTION,LTEST)
C
C  THIS SUBROUTINE CALCULATES A MACH NUMBER GIVEN A CHOKED
C          LENGTH DISTANCE
C          FOR FANNO FLOW
C
      REAL M1,M2,DELTAM,LTEST,LSTAR2
      IF(M1.GT.1.0)GOTO 121
      DELTAM = 0.1
      GOTO 122
121   DELTAM = -0.1
122   M2 = 1
120   M2 = M2 - DELTAM
      COEFA = (1 - M2**2)/(GAMMA * M2**2)
      COEFB = (GAMMA + 1)/(2 * GAMMA)
      COEFC = (GAMMA + 1) * M2**2
      COEFD = 2 * (1 + ((GAMMA - 1)/2 * M2**2))
      ARG = COEFA + COEFB * LOG(COEFC/COEFD)
      LTEST = DIA * ARG/FRICTION
      IF(LTEST.LT.LSTAR2)GOTO 120
      IF(ABS(DELTAM).LT.0.0001)GOTO 130
      M2 = M2 + DELTAM
      DELTAM = DELTAM * 0.1
      GOTO 120
130   RETURN
      END
C
```

```
      SUBROUTINE FRICFRAC(FRICTION,RE,ROUGH)
C
C   THIS SUBROUTINE CALCULATES THE FRICTION FACTOR (FROM
C     MILLER)
C   FOR TURBULENT PIPE FLOW GIVEN THE REYNOLDS NUMBER AND
C    SURFACE ROUGHNESS
      REAL FRICTION,RE,DELTAF,X,ROUGH
      FRICTION = 950.001
      DELTAF = 50.0
 700  FRICTION = FRICTION - DELTAF
      X=SQRT(FRICTION)*((-0.86859)*
     & LOG((ROUGH/3.7)+(2.51/(RE*SQRT(FRICTION)))))
      IF(X.GT.1.0)GOTO 700
      FRICTION = FRICTION + DELTAF
      DELTAF = DELTAF * 0.1
      IF(DELTAF.LT.0.00001)GOTO 710
      GOTO 700
 710  CONTINUE
      RETURN
      END
```

# Appendix II

AIAA 94-0335

# LEAK DETECTION METHODS FOR SPACECRAFT-BASED CRYSTAL GROWTH FURNACES

Valerie M. Belcher
Daniel W. Mackowski
Roy J. Hartfield, Jr.
and
Sushil H. Bhavnani
Auburn University

32nd Aerospace Sciences
Meeting & Exhibit
January 10-13, 1994 / Reno, NV

# LEAK DETECTION METHODS FOR SPACECRAFT-BASED CRYSTAL GROWTH FURNACES

Valerie M. Belcher,[§] Daniel W. Mackowski,[†] Roy J. Hartfield, Jr.[‡] and Sushil H. Bhavnani[*]
Auburn University, Al 36849

## Abstract

A survey has been conducted to evaluate potential leak detection methods for current and future crystal growth furnaces designed for use aboard the space shuttle and the space station. Analyses estimating the effectiveness of methods determined to be practical for such an application were performed and are presented herein. Some requirements for the implementation of the detection techniques have been determined from these analyses.

## Introduction

Recent interest in the field of microgravity science has prompted the development of devices, such as the Crystal Growth Furnace (CGF), to fully capitalize on the microgravity ($\mu$g) environment on board the National Aeronautics and Space Administration's (NASA) space shuttle. A modular, rack-mounted facility, the CGF is used to determine how the absence of gravity-driven convection affects vapor transport and directional solidification processes. Many of the crystal materials used on previous flights and those planned for future missions are both extremely toxic (i.e. Hg, As, Cd), and have significant vapor pressures at the processing temperatures. These characteristics affect the implementation of crystal growth experiments on future shuttle flights, and possible long-term experimentation on board Space Station Freedom (SSF).

Originally, the CGF was located in the cargo bay of the shuttle. Not being environmentally contained within the crew's atmosphere, leakage of the toxic species was of little concern. Yet eventually, as various flight modifications took place, the CGF was moved to a location inside the Spacelab module where it would require manual manipulation by the crew. Leak detection and species containment have now become paramount concerns, as exposure to such compounds could be lethal. Additionally, deposition of the crystal compounds onto CGF instrumentation could necessitate costly repairs, potentially involving the return of the assembly to earth.

The CGF is a reusable facility capable of processing up to six crystal growth samples automatically, at temperatures reaching 1600 °C. The main element of the CGF, the Integrated Furnace Experiment Assembly (IFEA), consists of the Experiment Apparatus Container (EAC), a mechanical Sample Exchange Mechanism (SEM) that rotates a new sample into position, and a Reconfigurable Furnace Module (RFM). A schematic of this configuration is shown in Fig. 1.

In addition to furnishing the primary structural support, the EAC provides containment for the argon gas atmosphere and houses the internal experiment hardware. A sample insertion port is included on the EAC for manual sample exchange for missions where more than six samples are scheduled.

In the current design, the samples are contained within a quartz ampoule which, in turn, is secured inside a thin metal cartridge. The sample/ampoule cartridge assembly (SACA), shown in Fig. 2, is held immobile by the SEM while the furnace is vertically translated over the sample being processed, thus avoiding any acceleration-induced defects during crystallization. In addition, the system allows precise control of melting and crystal growth conditions.

The furnace is comprised of a hot zone, an insulated or adiabatic zone, and a cold zone. The center 14 cm of the cold zone and the center 20 cm of the hot zone, both measured in the radial

[§] Research Assistant, Mechanical Engineering

[†] Assistant Professor, Mechanical Engineering

[‡] Assistant Professor, Aerospace Engineering, Member AIAA

[*] Associate Professor, Mechanical Engineering

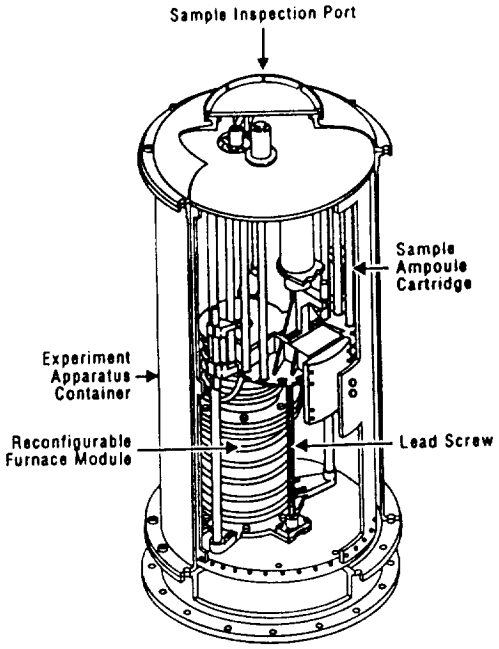


**Figure 1**: Integrated Furnace Experiment Assembly (From Ref. 1)

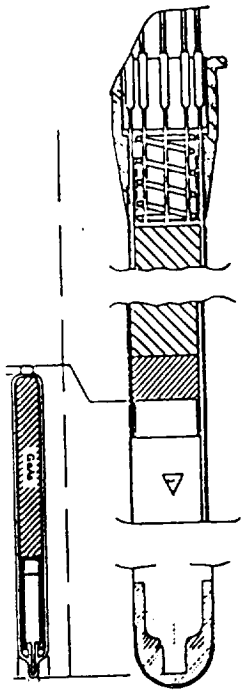

**Figure 2**: Sample/Ampoule Cartridge Assembly (Adapted From Ref. 2)

direction, are isothermal to ±1.0%, preventing appreciable discontinuity of heating within a sample. The RFM may be modified between flights by changing the adiabatic zone length to create different heating gradients.

In accordance with current safety certification requirements, the CGF facility has three levels of containment: the combined SACA, the negative pressure in the EAC relative to the Spacelab environmental pressure, and the EAC. Although this provides three distinct levels of fault tolerance, the design has several limitations. First, there is no method of detecting the failure of an individual ampoule and/or its cartridge. Thus, if processing were to occur on a failed SACA, the elevated processing temperatures would serve to volatilize the sample, possibly driving the material out into the EAC if an escape route exists. Second, the current method to detect sample materials in the EAC is by visual inspection of vapor deposition on a reflecting plate. This method cannot distinguish between the deposition of hazardous materials released from the ampoules and benign substances outgassed or condensed from furnace materials.

One factor constraining the use of more elaborate failure detection techniques is the limited space available within the furnace assembly. Most of the volume inside the EAC is filled with the furnace, the translation system, and the SEM. Additionally, the cartridges for the Marshall Space Flight Center (MSFC) version of the experiment are 59.16 cm long, with 16.00 to 28.43 cm of that envelope being occupied by an ampoule. Any method of failure detection located within the cartridge would need to be extremely compact and, depending on its location with respect to the ampoule, able to withstand high temperatures. Equally important is that a potential failure detection system not present a safety hazard in itself, and that it not adversely affect the crystallization process.

This paper focusses on finding possible solutions to the current safety problems resulting from a leakage of the toxic compounds from the CGF. Any method used to accomplish this task must adhere to current NASA safety specifications and regulations, as well as meet the experiment specific criteria mentioned in the previous paragraph. In addressing these issues, the investigation has focussed on identifying methods for sensing both ampoule failure and cartridge

failure, and for quantitatively detecting the presence of sample vapors within the EAC. The effectiveness of leak detection methods that rely on the direct sensing of sample materials are evaluated, and detection times are estimated.

## Literature Review

The literature reviewed during the course of this investigation covered various detection methods, including instrumentation and principles of operation, as well as NASA documentation defining the specific parameters and requirements for the CGF experiment.

Among the detection methods, atomic emission spectroscopy and its recent advances was reviewed by Beauchemin et al.[3] for Analytical Chemistry. In addition to providing numerous background sources, the review covered sampling techniques, excitation sources, detection systems, and data processing in detail. In the area of tracer technology, Dietz and Senum[4] discussed the selection of gaseous tracers, their applications, and sampling instrumentation. Similarly, a review of radiotracer theory and selection was conducted by Foldiak,[5] while Kleinknecht[6] examined numerous radiation detection devices. Other detection methods investigated include the following: fiber optic gas sensing, a brief review of which was conducted by Moslehi et al.;[7] ultrasonic testing, comprehensively detailed in a series of reviews edited by Szilard;[8] fiber optic pressure sensing, explained by Saaski et al.;[9] and a make-wire sensor, detailed by Johnson and Galloway[10] in a NASA disclosure of invention.

Additionally, several NASA documents were reviewed to obtain specific information on the CGF facility and requirements governing its operation. They include the following: parameters for each of the four crystal growth experiments flown on USML-1 were found in NASA/MSFC documents ICD-2-60026 through ICD-2-60029;[2,11-13] a detailed system design description was given in NASA/TBE SP-DOC-6102;[1] safety requirements concerning the release of hazardous chemicals were listed in NASA/JSC NSTS-1700.7B;[14] and data used to determine temperature profiles within the cartridge was found in NASA/TBE SP-RPT-6752[15] and TBE memorandum MEPF-CGF 2/93-311.[16] Since CGF materials and processing requirements are likely to be similar on future flights, the information contained in these documents was used as the basis for the analyses contained in this report.

A comprehensive review on the preparation of crystal growth materials and the dependence of the material properties on preparatory conditions was edited by Wilcox.[17] Further data regarding the volatile species and their vapor pressures was found in the NASA documents listed above and The Handbook of Chemistry and Physics.[18] Relations for the Fanno flow analysis discussed in section 4.2 were adapted from Shapiro[19] and Miller.[20]

## Failure Detection Methods

Although numerous detection methods were examined during the course of this investigation, most were eliminated due to insufficient technological development or an inability to work within the special constraints of the CGF system. For example, mass spectrometry and gas chromatography are proven gas analyzation techniques, but are too cumbersome to be easily deployed within the EAC environment. Various tracer techniques were also considered, but were limited in that they could not specify which SACA had failed. Additionally, specific gas sensing through the use of fiber optics or electrochemical devices has not yet reached a level of development that would facilitate their use with crystal growth species.

A few detection methods, however, did show promise for CGF applications. One of these, a make-wire sensor is employed to qualitatively detect crystal growth species inside the cartridge in the event of an ampoule failure. In principle, a small gap in the sensor is closed by the deposition of sample vapor, thereby giving finite resistance to a previously open circuit. Although initial testing has been successful in demonstrating the feasibility of the method, the sensor has not yet been tested under flight conditions. Additionally, a determination as to whether the outgassing of other materials in the SACA would produce a false positive detection needs to be made.

Detecting a cartridge failure and possibly an ampoule failure by means of pressure measurement was also investigated. Several commercially available piezoresistive transducers are compact enough to fit within the cartridge, and sensitive enough to detect minute pressure variations. Another commercially available option uses a fiber optic sensing system based on spectral modulation. The sensor, a thin diaphragm stretched

over a shallow cavity, flexes with changes in pressure, thus changing the back reflection of the optic. Although uniquely suited for use in hazardous environments, at 0.7 kPa, the resolution of the system is somewhat less than that of standard transducers.

In the event of a combined ampoule/cartridge failure resulting in the release of sample materials into the EAC, spark source emission spectroscopy techniques could be utilized to detect the sample species in sub-parts per million concentrations. Each metallic element emits radiation at characteristic wavelengths, and, given that each ampoule contains a slightly different composition, it would be possible to determine precisely which SACA has failed. Primary disadvantages associated with the method include the sizable instrumentation requirements and the high-voltage spark used as the excitation source.

## Thermodynamic Analysis

An ampoule failure will result in two occurrences: the deposition of sample material onto the cartridge walls and packing, and an increase in the total cartridge pressure. A simple thermodynamic analysis was conducted to determine where such an escaped species would deposit, and how great of a pressure increase could be expected.

Upon failure of an ampoule during processing conditions, the volatile component or components of the sample compound will vaporize and diffuse into the cartridge. Since diffusion can be assumed to be the limiting mechanism in removing the vapor from the surface of the sample, the vapor pressure at the surface will be the equilibrium vapor pressure of the volatile component above the compound for the given temperature conditions. This pressure can be substantial for the experiments flown on USML-1. For example, the vapor pressure of As above GaAs at the melting point was estimated, for the specific experimental conditions, at 2.24 atm. For HgCdTe the vapor pressure of Hg during the experimental processing is 9.46 atm.

Diffusion will eventually bring the vapor into lower-temperature regions of the cartridge. Deposition of the vapor will occur at the point in the cartridge that is at a temperature lower than the prevailing dew point temperature of the vapor. To predict the dew point temperature, we use a Clausius-Clapeyron relation of the form

$$\log P = \frac{a}{T_{dp}} + b \qquad (1)$$

where P is the vapor pressure of the volatile component over the sample and a and b are constants specific to the component. To give an indication of the behavior of the vapor in the cartridge, the estimated temperature profile during processing for the HgCdTe experiment flown on USML-1 is shown in Fig. 3, in which distance is measured from the cartridge cap. The dew point

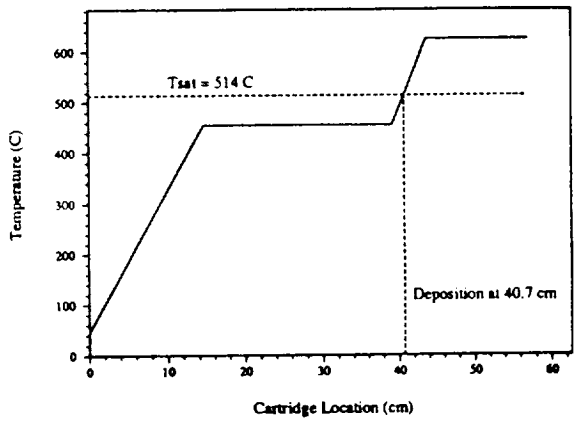


**Figure 3:** Temperature Profile for USML-1 Experiment (HgCdTe)

temperature for that sample species and its relative location within the cartridge are indicated with the dashed lines. From this figure, it is apparent that the point of deposition of the escaped species is located at 40.7 cm measured from the cartridge cap. Similar plots for each of the USML-1 experiments show deposition locations ranging from 2.3 cm for GaAs to 43.6 cm for HgZnTe. These results are highly dependent on both the temperature profile within the cartridge and the specific sample being processed. Thus, if an experiment were at a different point in its processing stage, the temperature profile, and subsequently, the point of deposition, would change. Additionally, since the dew point temperature is specific to a given species, any two experiments with the same temperature profile but different samples would have different deposition locations.

The increase in cartridge pressure resulting from an ampoule failure was calculated by summing the increase in mass within the cartridge due to the escaped species. The argon already present within

Table 1: Changes in Cartridge Pressure due to Ampoule Failure for USML-1 Processing Conditions

| | HgCdTe | GaAs | CdZnTe | HgZnTe |
|---|---|---|---|---|
| $P_{cart,proc}$ (kPa) | 101.33 | 227.53 | 101.33 | 101.33 |
| $\Delta P$ (kPa) | 218.7 | 171.0 | 42.1 | 457.7 |
| % increase | 216% | 75% | 42% | 452% |

the cartridge was assumed to be displaced by the sample. The following equation, derived from ideal gas law, was used to estimate the change in cartridge pressure:

$$\Delta P = \frac{T_c}{V_c} \int \frac{P(x)}{T(x)} A(x)dx \qquad (2)$$

where $T_c$ is the weighted average temperature of the cartridge, $V_c$ is the total cartridge volume, P(x) and T(x) are the local vapor pressure and temperature of the sample, and A(x) is the open cross sectional area of the cartridge at that location. The open cross sectional area for each cartridge was estimated using a NASA engineering drawing of that SACA. P(x) was assumed to be the vapor pressure of the volatile component above the compound until the temperature fell below the dew point temperature for which P(x) was calculated using the Clausius-Clapeyron equation specified above. The changes in cartridge pressure due to an ampoule failure were calculated at processing conditions for each sample flown on USML-1, and are summarized in Table 1.

## Pressure Sensitivity Analysis

A pressure sensitivity analysis was conducted to estimate the response times of a detection method based on pressure measurement in the event of a cartridge failure. A hole in the wall of the cartridge was modeled as a converging nozzle on the inside of the cartridge, in series with a duct through the wall opening to the EAC environment. Flow through the nozzle was assumed to be isentropic, and Fanno flow relations were used through the duct.

A computer program was used to solve the relations, using an iterative approach until specified conditions at the duct exit were satisfied. A selection between two exit conditions was determined by comparing the Fanno length L* (the length necessary for choked flow through the duct) to the actual duct length. The rules employed in the selection are as follows. If L* was less than or equal to the duct length, the Mach number at the exit was set equal to one. For the case where L* was greater than the duct length, the iteration was continued until either the exit pressure equaled the back pressure, or the value of L* decreased to the duct length. A Colebrook friction factor was used, based on the Reynolds number at the duct entrance and the pipe roughness.

The time required for the cartridge pressure to change by a specified percent was then calculated by combining the definitions of mass flow rate and the ideal gas law to yield:

$$\Delta t = \frac{V}{\dot{m}RT_o} \Delta P_o \qquad (3)$$

where $\Delta t$ is the time in seconds, V is the flow velocity at the duct entrance, $\Delta P_o$ and $T_o$ are the change in cartridge pressure and the temperature within the cartridge respectively, $\dot{m}$ is the mass flow rate through the duct, and R is the gas constant for argon.

Calculations were performed for each of the experiments flown on USML-1, using processing conditions. An example plot showing response times as a function of hole diameter is shown in Fig. 4. Table 2 contains some response times for selected hole diameters for a $\Delta P/P$ of 2.0%.

For three out of the four cartridges flown on USML-1, the internal cartridge pressure during processing reached 101.3 kPa. During this time interval, the EAC pressure was maintained at 96.0 kPa. Increasing the pressure differential across the cartridge and EAC would obviously decrease the time required for a specified change in cartridge pressure. Calculations of the response times were therefore performed for one of the cartridges using different internal pressures. The HgZnTe cartridge

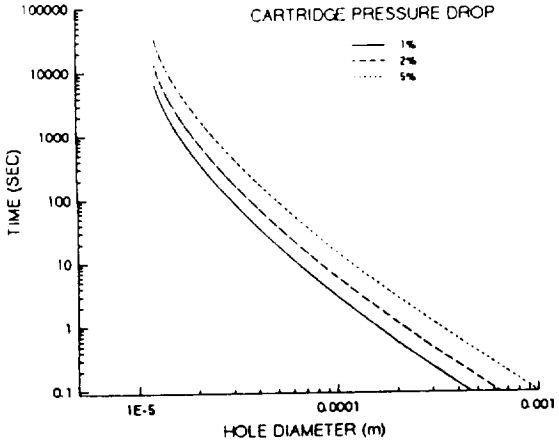


**Figure 4**: Response Times for Cartridge Leaks Based on the HgZnTe Experiment Flown on USML-1.

flown on USML-1 was chosen for this example calculation. Results demonstrated an 82% decrease in detection time when decreasing the original internal cartridge pressure at processing conditions by only 18.6 kPa. These calculations are briefly summarized in Table 3.

## Discussion

The results of the thermodynamic analysis highlight two issues of vital importance to safety considerations regarding the SACA . First, the success of any leak detection method based on sample deposition is dependent on its location within the cartridge. For instance, the make-wire sensor would need to be located at a position where the temperature in the cartridge reaches the dew point temperature of the volatile species. If the sensor is at a temperature higher than the dew point, the sample vapor will not deposit, and therefore not be detected. Conversely, if the sensor is located at a temperature below the dew point, but at a position far enough removed from where that temperature is first reached, the species could deposit out onto the cartridge walls and packing, and thus never reach the sensor. An additional complication to this positional sensor dependence is that the location of the dew point temperature within the cartridge varies with time as the furnace is translated during processing. Any deposition sensor would therefore need to be positionally independent. For example, a sensor would need to be fabricated in the form of a continuous strip running the length of the cartridge instead of a miniaturized, discrete unit.

Another safety concern resulting from the thermodynamic analysis, is the magnitude of the pressure increase within the cartridge in the event of an ampoule failure. For one sample, an ampoule failure resulted in a 400% increase in cartridge pressure at maximum processing conditions. Cartridge integrity under these circumstances needs to be assured. One advantage to such a pressure increase, however, is that it would be easily detectable by a pressure measurement technique.

Additionally, the pressure sensitivity analysis demonstrates that response times for

Table 2: Response Times (sec) for $\Delta P/P$ = 2% for Selected Hole Diameters

| Diameter (mm) | HgCdTe | GaAs | CdZnTe | HgZnTe |
|---|---|---|---|---|
| 0.014 | 3,640 | 29.0 | 6,310 | 3,860 |
| 0.1 | 4.7 | 0.2 | 3.8 | 5.6 |
| 1.0 | 0.03 | <0.01 | 0.02 | 0.04 |

Table 3: Response Times (sec) for Various Cartridge Pressures for the USML-1 HgZnTe Experiment

| Diameter (mm) | 101.33 kPa | 82.74 kPa | 68.95 kPa | 55.16 kPa |
|---|---|---|---|---|
| 0.012 | 13,500 | 2,430 | 966 | 561 |
| 0.1 | 5.6 | 3.1 | 1.9 | 1.3 |
| 1.0 | 0.04 | 0.02 | 0.01 | 0.01 |

detecting a cartridge failure can be significantly reduced by increasing the pressure differential across the cartridge to the EAC. Creating such a negative cartridge pressure differential with respect to the EAC would be desirable in terms of a cartridge level of containment. However, in the event of an ampoule failure, the cartridge pressure would be much greater than that of the EAC. This means that a species escaped from an ampoule would still be driven out of the cartridge should the cartridge also fail, despite a reduced cartridge internal pressure. Therefore, reducing the cartridge internal pressure would serve to reduce the response time for detecting cartridge failure, but would not likely be of any benefit were the ampoule to also fail.

## Conclusions

In summary, any ampoule failure detection method based on sample deposition needs to be able to withstand the maximum processing temperatures of a sample, since it will need to detect a crystal growth species at any point along the length of the cartridge. Any such method must also demonstrate an ability to withstand outgassing by other SACA materials, such as thermocouples, without yielding false positive detection results. Additionally, while a pressure measurement detection method would appear to effectively warn of a cartridge or ampoule failure, one issue needs to be addressed. Since the pressure within the cartridge increases with increasing temperatures during processing, a supporting code would need to be incorporated to define the normal parameters of this increase, and warn of a failure only when the cartridge pressure falls outside this range. The accuracy of such a code would also be dependent on the reliability of the heating rate within the furnace.

## Acknowledgement

This work has been supported by the NASA Marshall Space Flight Center under contract NASA-NAS8-39131-D06, I. C. Yates technical monitor.

## References

1. Teledyne Brown Engineering: SP-DOC-6102, "Design and Development of the Multiple Experiment Processing Furnace: System Design Description," Contract Number NAS8-36637, March 1990.

2. NASA/MSFC: ICD-2-60026, "CGF Experiment Cartridge Interface to the P.I. Sample/Ampoule Assembly — Crystal Growth of Selected II - IV Semiconducting Alloys by Directional Solidification," March 1990

3. Beauchemin, D.; Le Blanc, J.C. Yves; Peters, Gregory R.; and Craig, Jane M. "Plasma Emission Spectroscopy," Analytical Chemistry, Vol. 64, No. 12, June 1992, 442R-467R.

4. Dietz, R. N.; and Senum, G. I. "Capabilities Needs, and Applications of Gaseous Tracers," in: Atmospheric Tracer Workshop, Santa Fe, NM, May 21-25, 1984, Los Alamos National Laboratories, LA-10301-C, December 1984, 123-173.

5. Foldiak, G. (Editor): Industrial Applications of Radioisotopes, Elsevier Science Publishing Co., New York, 1986.

6. Kleinknecht, K.: Detectors for Particle Radiation, Cambridge University Press, Cambridge, 1986.

7. Moslehi, B.; Shahriari, M. R.; Schmidlin, E. M.; Anderson, M.; and Lukasiewicz, M. A. "Optical Fiber Simplifies Gas-Sensing Systems," Laser Focus World, April 1992, 161-168.

8. Szilard, J. (Editor): Ultrasonic Testing: Non-Conventional Testing Techniques, John Wiley & Sons, New York, 1982.

9. Photonetics, Inc., Fiber Optic Pressure Sensor Product Information, 1993.

10. Johnson, M.L., and Galloway, P.N.: Metal vapor or electronic semiconductor material sensor/detector. NASA disclosure of Invention, NASA/MSFC, 1990.

11. NASA/MSFC: ICD-2-60027, "CGF Experiment Cartridge Interface to the P.I. Sample/Ampoule Assembly — The Study of Dopant Segregation Behavior During Growth of GaAs in Microgravity," March 1990.

12. NASA/MSFC: ICD-2-60028, "CGF Experiment Cartridge Interface to the P.I. Sample/Ampoule Assembly — Vapor Transport Crystal Growth of HgCdTe in Microgravity," March 1990.

13. NASA/MSFC: ICD-2-60029, "CGF Experiment Cartridge Interface to the P.I. Sample/Ampoule Assembly — Orbital Processing of High Quality CdTe Compound Semiconductors," March 1990.

14. NASA/JSC: NSTS 1700.7B, "Safety Policy and Requirements for Payloads Using the Space Transportation System," January 1989.

15. Teledyne Brown Engineering:2 SP-RPT-6752, "Design and Development of the Multiple Experiment Processing Furnace: Reconfigurable Furnace Module Thermal Analysis Report," Contract Number NAS8-36637, April 1991.

16. Teledyne Brown Engineering: Memorandum MEPF-CGF 2/93-311, "Ampoule Positions and Temperatures for USML-1," Shelly LeRoy to Srini Srinivas, October 15, 1993.

17. Wilcox, W. R. (Editor), Preparation and Properties of Solid State Materials, Volume 2, Marcel Dekker Inc., New York, 1976.

18. Handbook of Chemistry and Physics, 73rd Edition, Chemical Rubber Publishing Co., Boca Raton, Florida, 1992-1993.

19. Shapiro, A. H., The Dynamics and Thermodynamics of Compressible Fluid Flow, John Wiley & Sons, New York, 1953.

20. Miller, R. W., Flow Measurement Engineering Handbook, McGraw Hill, New York, 1983.